RESEARCH ARTICLE

Risk Management in Solar Power Plants with Storage: A Comparative Study

Fernando S. Oliveira[a] and Carlos Ruiz[b]

[a] Agriculture and Trade Department, OECD, 2, rue André Pascal, 75775 Paris CEDEX 16, France; [b] Department of Statistics & UC3M-BS Institute for Financial Big Data (IFiBiD), University Carlos III de Madrid, Avda. de la Universidad, 30, 28911-Leganes, Spain

ARTICLE HISTORY
Compiled March 10, 2026

ABSTRACT
Using risk-averse stochastic programming, we study the management of solar power plants considering trading in the spot and future markets, together with storage systems and a novel weather derivative based on solar radiation. We compare the performance of two main solar-based technologies: a concentrated solar power plant with thermal storage (CSP) and a photovoltaic power plant with electrical batteries (PV). The methodological contribution is the study of the interaction between energy trading, weather derivatives and storage under risk aversion. The managerial contributions are the following. First, we analyze the interaction between optimal trading and storage. Second, we unveiled how the value of the put and call options depends on solar radiation, generation, and storage levels. Moreover, we have shown that the optimal strategy is to sell calls and buy put options and that generators with a storage system sell significantly more call options. Third, we proved that the higher the risk aversion, the more the generator sells in the futures market and the higher the number of purchased put contracts. Finally, by using numerical analysis to compare CSP and PV plants, we show that PVs are more profitable under the considered conditions and that batteries create more value.

KEYWORDS
Energy Storage, Renewable Energy, Risk Management, Sustainability, Weather Derivatives.
SDG 7: Affordable and clean energy.

1. Introduction

The energy sector is vital in reducing CO_2 emissions. One of the current trends is to electrify as many industrial activities as possible and, in parallel, generate this electricity with carbon-free energy sources. Governments worldwide are proposing market mechanisms to encourage these investments and accelerate the energy transition. For example, the EU Emission Trading System (EU-ETS) aims to achieve a net reduction

CONTACT Fernando Siciliani Oliveira. Email: fernando.deoliveira@oecd.org. The data that support the findings of this study are available from the corresponding author, F.S. Oliveira, upon reasonable request.

C. Ruiz gratefully acknowledges the financial support from MCIN/AEI/10.13039/501100011033, project PID2020-116694GB-I00 and from the Madrid Government (Comunidad de Madrid) under the Multiannual Agreement with UC3M in the line of "Fostering Young Doctors Research" (ZEROGASPAIN-CM-UC3M), and in the context of the V PRICIT (Regional Programme of Research and Technological Innovation)

CO_2 of emissions of 55% by 2030 and climate neutrality by 2050 (EC Climate Action 2022), which requires the massive deployment of clean energy sources.

However, high levels of renewable energy penetration present technical issues as it substantially decreases system reliability. This effect is especially significant with the extensive deployment of photovoltaic (PV) plants. For example, some critical hours within a day (sunset in the late afternoon) when PV generation dramatically decreases, and dispatchable plants (usually gas-fired plants) must be ramped up or turned on to cover the demand loads. This can significantly compromise the correct operation of the network and sustain the dependency on carbon-based generation technologies.

Therefore, this transition requires the massive installation of clean and renewable resources and the promotion of technologies that foster their dispatchability. This can be achieved by deploying large-scale energy storage systems that can be charged or discharged depending on the load needs and the availability of renewable resources. There are some centralized large-scale storage solutions: pumped hydropower, compressed air, large-scale batteries, flywheels, etc. However, most are still under development to improve reliability and decrease investment costs. Another storage alternative, which is gaining attention these days, is to endow each renewable generation plant with storage capabilities so they can tackle and soften the variability of renewable generation locally.

With this motivation, we are particularly interested in the case of two prominent solar-based technologies with storage. First, we analyze the Concentrated Solar Plants (CSPs). These are flexible and sustainable and contribute to the electricity system's reliability (World Bank 2021). This technology concentrates solar radiation with mirrors in a Solar Field (SF) to heat a transfer fluid (molten salt or oil), which generates steam and moves a turbine to produce electricity. Its main advantage is integrating a relatively low-cost storage system for the heated fluid so that electricity generation can be scheduled for hours without sunlight. Hence, CSPs can provide stability to the grid in scenarios of high penetration of renewable energy. In addition, CSPs present generation costs similar to those of combined cycle gas plants, their main competitors in the market for flexible dispatching. The most recent CSP plants have been built in Chile, China, Morocco, and the United Arab Emirates, and many others are planned to be installed in the coming years, e.g., in Spain, the government announced a plan to build an additional 5GW of CSP by 2030, more than tripling the 2.3GW installed in 2020 (World Bank 2021).

Second, we study PV Power Plants (PVs) with electrical batteries. PVs are the energy production technology proliferating worldwide, increasing from 137 GW in 2013 to more than 1000 GW in 2022 (IRENA 2023). This growth is expected to continue in the short- and medium-term. For instance, Europe has plans to reach 320 GW by 2025 and 600 GW by 2030 (REPowerEU 2022). Moreover, a significant trend is to incorporate a medium-size battery storage system, primarily based on lithium-ion cells (Hannan et al. 2021), to the new PVs so that they can cope with the daily variability of the solar irradiation and increase the system reliability. These technologies have become very competitive in cost compared to other renewable or fossil-based production and storage technologies (IRENA 2022).

However, the profitability of these units is still highly dependent on effective financial instruments, as they are exposed to high levels of uncertainty. These include uncertain market outcomes and renewable resource availability, i.e., quantity risk. This article analyzes how standard futures and spot trading complement a physical storage system and weather derivatives to mitigate quantity and price risks. In particular, we are interested in studying solar radiation-based derivatives, as they directly link

weather conditions with power plant energy production, which potentially has important implications for their risk management. These financial instruments are seldom traded, but they are a growing market segment and specifically designed for solar power plants. Even though most options and futures trading in practice are based on temperature and catastrophic events[1], with enhanced data availability, the design of financial instruments based on solar radiation will be more common, as they better track the risks faced by solar power plants (and other businesses dependent on solar radiation). For example, Munich RE proposes trading swap contracts based on solar radiation[2]. The Iberian market trades financial derivatives based on electricity and gas, including futures, options, and swap contracts[3].

In the formulation of this model, we characterize a two-stage process where decisions are sequentially taken over time. The first-stage is a long-term contract, either a forward contract (over-the-counter), a futures contract, or a power purchasing agreement. For this reason, even though we use mostly futures markets to indicate this first-stage for the remainder of the paper, it should be interpreted as a long-term contract that fixes the electricity price.

In particular, the power plant trades in a futures market (physical) and on weather-related option contracts (first stage); afterward, the plant sells and buys the excess remaining energy in a spot market (second stage) where the delivery of the power committed in the futures also takes place. Hence, the first-stage decisions are accepted subject to different sources of uncertainty in the second-stage, including hourly spot prices and solar radiation. The second-stage decisions are taken once these uncertainties are resolved at the spot market.

To address this problem, we propose a two-stage stochastic optimization approach solved by backward induction to address this problem. The second stage is analyzing the decisions first, i.e., how much to generate and store and how much to sell or buy in the spot market. The first stage decisions are analyzed last, i.e., how much to buy and sell in the futures markets (physical) and how much to buy and sell in weather options (financial). The plant maximizes the profit's Conditional Value at Risk (CVaR). The analysis also considers different representative seasons (Winter and Summer) to explain better how the plant operates under diverse weather conditions.

The CVaR is extensively used to analyze decision-making under risk aversion. Its mathematical properties allow its implementation in significant computational problems tackled with linear programming techniques (e.g., Rockafellar et al. 2000). In the context of energy markets and renewable energy, the CVaR has been used to analyze risk management under uncertainty (Conejo et al. 2010), procurement in electricity markets with futures and spot contracts (Oliveira and Ruiz 2021), and petroleum markets considering futures, spot and swap contracts (Oliveira 2023).

Solar-based electricity generation is exposed to high uncertainty levels, including price volatility and solar radiation availability. The research questions addressed in this article are the following. How can energy storage be used for risk hedging? How can futures and spot trading mitigate quantity and price risks? Is there a role for solar radiation derivatives in quantitative risk management? How do the two solar generation technologies compare regarding operational decisions, financial performance, and risk management?

From a methodological perspective, the article significantly contributes by integrating CVaR with weather derivatives on solar power, considering energy storage. The

[1] https://www.cmegroup.com/
[2] https://www.munichre.com
[3] https://www.omip.pt/

article proposes the design of option contracts on solar radiation that can be used with futures and spot contracts in risk management. Moreover, even though focusing on solar power, this risk management framework can be adapted and applied to the operation of any other renewable generating technology with quantity risk from an uncertain energy source (wind, hydro, etc.) and with some storage capabilities.

From a policy perspective, the significant contribution is to analyze the interaction between futures and spot trading, weather options prices and trading, and storage in determining the best price and quantity risk management strategy. Moreover, we have compared the performance of PVs and CSPs regarding operational decisions, production trading strategies, risk management, and profitability.

2. Literature Review

Integrating renewable energy, which is non-dispatchable and has low operational costs, into the electricity system is an important research topic. For example, the interplay between optimal investment of renewable and conventional power plants, with particular attention to operational flexibility, is analyzed by Kök et al. (2020). They show that subsidies for gas-fired plants can incentivize investment in solar power plants.

Motivated by these renewable plants' uncertain and intermittent available capacity, some articles analyze and propose specific hedging tools. In this regard, Bhattacharya et al. (2020) explores hedging strategies for a solar-based power producer with temperature-based weather derivatives. The simulations show how the level of risk increases during the fringe summer and winter periods. In a bargaining and risk-averse context, Gutjahr et al. (2022) shows how a shared solar plant's optimal investment and management can be reached by exchanging standard call and put options. Li et al. (2020) proposes to combine real options and stochastic dynamic programming to derive adequate feed-in tariffs that promote renewable investments. With a focus on wind power generation, Peura and Bunn (2021) investigates how intermittent renewable sources may impact electricity prices when forward markets are available. They show how there is a threshold of renewable capacity upon which hedging forward decreases, resulting in higher spot prices. A multi-stage stochastic program is developed to show that, for the low-price impact assets, participating in the first auction is less relevant than in the subsequent one. From an operational perspective, Guajardo (2018) empirically compares direct vs. third-party solar energy systems ownership. They implement an econometric random-effect model to show that third-party ownership presents better performance. Feng and Menezes (2022) shows how production systems can significantly benefit from adopting renewable generation technologies combined with energy storage.

In this article, we seek to investigate additional hedging tools for new types of flexible generating plants, combining a renewable source and an energy storage system. We focus on CSP and PVs plants, which can be relevant in decarbonizing the future electricity sector.

In general, solar-based power plants integrating storage require high investment costs, but once built, they allow for a flexible operation with low generation costs production. This is the case of CSPs, for which an appropriate economic and technical assessment is critical to evaluate their pros and cons. In particular, Dowling et al. (2017) analyzes different metrics and shows how, for CSPs, policy and investment decisions must account for flexibility and time-varying effects. Another essential aspect of CSP plants is their optimal operation, as they combine different technologies and

are subject to renewable availability and market uncertainties.

Similarly, PVs are being deployed massively, reaching significant shares of generation capacity in power systems worldwide (IRENA 2023). However, this requires battery-based storage to increase the systems' flexibility and dispatchability. Lai et al. (2017) presents a revision of the technical properties of integrated large-scale photovoltaic and storage systems and their main operating characteristics. Similarly, Hernández-Callejo et al. (2019) highlights critical challenges associated with the design, operation, and maintenance of photovoltaic systems. Focusing on the battery storage systems, Hannan et al. (2021) revises the main solution approaches for their optimal sizing and allocation, attending to cost, capacity, and power quality objective functions, with their main operational constraints. Chen et al. (2024) studies the integration of PVs and batteries in industrial manufacturing environments. Results show that this combination and a grid-responsive operation of the industrial process can significantly reduce monetary costs and emissions.

To determine the optimal size and technical properties of a PV plant with storage, Merzifonluoglu and Uzgoren (2018) proposes a stochastic linear optimization problem that includes the CVaR to account for the cost risk. A sample average approximation method incorporates load, power output, and system performance uncertainties into the model. (Keles and Dehler-Holland 2022) assess the economic profitability of large-scale PV systems with storage under price and production uncertainty. The operations are modeled as a Markov decision process, solved with stochastic dynamic programming techniques. It is shown how combining PV and storage in large power plants can significantly improve their profitability and justify investments, especially under high price volatility levels. Fan et al. (2023) proposes a two-stage setting combining a multi-objective RES scheduling approach and a data-driven dynamic emission model. The system incorporates energy storage technologies, which optimally allocate loads and reduce total costs and emissions.

As we have discussed, two significant uncertainties affect general renewable power plants: price and quantity (generation). Price risk can be managed using financial options on the electricity price, e.g., (Broadie and Detemple 2004). However, these financial options are not adequate to manage quantity risk; instead, we need to use weather options, which use one of some of the following physical measures of the weather behavior, temperature, wind speeds, precipitation (e.g., Leggio 2007, Elias et al. 2014).

However, none of these articles explored how to design radiation options to hedge quantity risk in power generation, primarily how these will interact with storage systems. They do not consider using CVaR to model risk aversion. Hence, in this work, we focus on filling this gap in the literature and studying effective financial instruments based on weather derivatives to increase the profitability of a new type of emerging technology: combining a renewable source with a storage system.

3. Description of the Mathematical Model

This section presents the decision-making optimization model for a general solar-based power plant with storage. The particular technology employed for the solar field and the storage system can be specified by an appropriate selection of the corresponding technical parameters (charging and discharging loss coefficients for the case of thermal or electrical storage, power conversion efficiencies, maximum and minimum storage capacities, maximum electricity generation capacities, etc.).

The power plant owner seeks optimal trading in the futures market and weather option trading to hedge the uncertainty of spot prices and solar radiation and maximize profit. This is achieved using the two-stage stochastic formulation (1), in which Ξ is the set of decision variables. All the notation is gradually introduced as we discuss the objective functions and constraints and summarized in the Online Appendix A for quick reference. Dual variables are indicated at their corresponding constraints following a colon. The Lagrangian and corresponding Karush-Kuhn-Tucker conditions for this problem are outlined in the Online Appendix B.

$$\underset{\Xi}{\text{Maximize}} \quad \text{CVaR} = \xi - \frac{1}{\alpha\Omega}\sum_{\omega} z_{\omega} \tag{1a}$$

subject to:

$$\Pi_{\omega} = FDq^{F} - D\sum_{o\in\mathbb{O}}\left(q^{c}_{o}c_{o} + q^{p}_{o}p_{o}\right) + \\ + \rho^{d}D\sum_{o\in\mathbb{O}}\left(q^{c}_{o}\sigma_{o}\left(R_{\omega}-R_{o}\right)^{+} + q^{p}_{o}\sigma_{o}\left(R_{o}-R_{\omega}\right)^{+}\right) + \rho^{d}\sum_{t}\Pi^{S}_{t\omega} \qquad \forall\omega \tag{1b}$$

$$\Pi^{S}_{t\omega} = S_{t\omega}q^{S}_{t\omega} - k_{t\omega}g_{t\omega} \qquad \forall t,\forall\omega \tag{1c}$$

$$-z_{\omega} + \xi - \Pi_{\omega} \le 0 \quad : \lambda_{\omega} \qquad \forall\omega \tag{1d}$$

$$-z_{\omega} \le 0 \qquad : \Phi^{z}_{\omega} \qquad \forall\omega \tag{1e}$$

$$q^{S}_{t\omega} \le \eta\left(g_{t\omega} + \beta\Delta_{-t\omega}\right) - q^{F} \qquad : \Phi^{S}_{t\omega} \qquad \forall t\in\mathbb{D},\forall\omega \tag{1f}$$

$$q^{S}_{t\omega} \le \eta\left(g_{t\omega} + \beta\Delta_{-t\omega}\right) \qquad : \Phi^{S}_{t\omega} \qquad \forall t\notin\mathbb{D},\forall\omega \tag{1g}$$

$$q^{F} \ge -q^{S}_{t\omega} \qquad : \Phi^{F}_{t\omega} \qquad \forall t\in\mathbb{D},\forall\omega \tag{1h}$$

$$\widetilde{E}_{t\omega} = g_{t\omega} + \Delta_{+t\omega} + E^{C}_{t\omega} \qquad : \Gamma^{E}_{t\omega} \qquad \forall t,\forall\omega \tag{1i}$$

$$b_{t\omega} = b_{t-1,\omega} + \beta\Delta_{+t\omega} - \Delta_{-t\omega} \qquad : \Gamma^{B}_{t\omega} \qquad \forall t\ge 2,\forall\omega \tag{1j}$$

$$b_{1\omega} = b_{T\omega} + \beta\Delta_{+1\omega} - \Delta_{-1\omega} \qquad : \Gamma^{B}_{1\omega} \qquad \forall\omega \tag{1k}$$

$$\underline{b} - b_{t\omega} \le 0 \qquad : \underline{\nu}_{t\omega} \qquad \forall t,\omega \tag{1l}$$

$$b_{t\omega} - \overline{b} \le 0 \qquad : \overline{\nu}_{t\omega} \qquad \forall t,\omega \tag{1m}$$

$$\Delta_{at\omega} - \Delta \le 0 \qquad : \delta_{at\omega} \qquad \forall a,t,\omega \tag{1n}$$

$$\eta\left(g_{t\omega} + \beta\Delta_{-t\omega}\right) \le \bar{q} \qquad : \Phi^{q}_{t\omega} \qquad \forall t,\omega \tag{1o}$$

$$-\Delta_{at\omega} \le 0 \qquad : \Phi^{\Delta}_{at\omega} \qquad \forall a,t,\omega \tag{1p}$$

$$-g_{t\omega} \le 0 \qquad : \Phi^{g}_{t\omega} \qquad \forall t,\omega \tag{1q}$$

$$-E^{C}_{t\omega} \le 0 \qquad : \Phi^{E^{C}}_{t\omega} \qquad \forall t,\omega \tag{1r}$$

Problem (1) is a large stochastic optimization model that is solved considering thousands of scenarios, variables, and constraints. Nonetheless, it is formulated as a linear optimization problem in all the decision variables so that it can be effectively solved by general-purpose optimization software. In particular, we employ CPLEX[4] under GAMS[5] to find the optimal solution to the different problems.

This problem includes four main modeling aspects: the profit risk, the technical operation of the plant, spot, and futures trading, and weather options, which are described in detail in the following sections.

[4]https://www.ibm.com/products/ilog-cplex-optimization-studio/cplex-optimizer.
[5]https://www.gams.com/

3.1. *Risk modeling*

The objective function (1a) represents the maximization of the profit CVaR, which is equivalent to the expectation over the $\alpha \times 100\%$ worst profit scenarios (Rockafellar et al. 2000; Rockafellar and Uryasev 2002), as represented in Figure 1. The level of risk aversion can be adjusted by using parameter $\alpha \in (0, 1]$: As α converges to 0, the degree of risk aversion increases; as α converges to 1, the generator becomes risk neutral. All scenarios $\omega = 1, \ldots, \Omega$ are considered equiprobable with a probability of $1/\Omega$. At the optimal solution of problem (1), the first term of (1a), i.e., ξ, is the profit VaR, while the second term represents the relative distance to the CVaR.

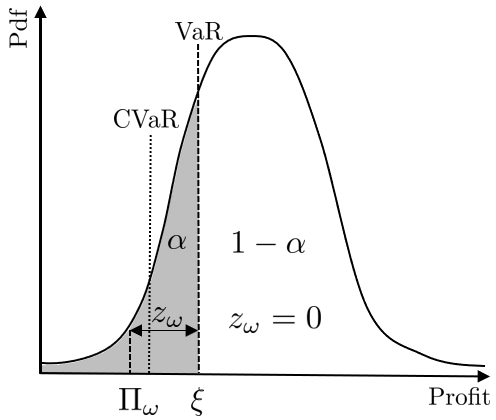

Figure 1.: CVaR of the profit function.

The total profit for each scenario ω is defined in (1b), where the first term represents the income from the futures market, i.e., from selling a quantity q^F, at a price F, during D periods. The second term is the contracting cost of the call (q^c_o) and put (q^p_o) options at premiums c_o and p_o, respectively. Note that $o \in \mathbb{O}$ refer to all available options for weather derivatives, such as solar radiation, for specific hours $t \in \mathbb{D}$. Specifically, we assume that $t \in \mathbb{D}$ refer to daylight hours, while $t \notin \mathbb{D}$, e.g., constraint (1g), to hours with no solar radiation. Finally, the third term in (1b) represents the profit from the spot market, discounted by a factor ρ^d. The hourly spot profit $\Pi^S_{t\omega}$ for each scenario ω and time t is defined by (1c). It is composed of income from the spot market (first term) minus generation cost (second term) plus income from exercising the call and put options (third and fourth terms, respectively). These are calculated in terms of the positive differences between the exercise radiation for an option o, i.e., R_o, and the average radiation R_ω, observed for each scenario ω, during the contract duration; the R_ω is calculated in equation (2), where $D = |\mathbb{D}|$ and represents the duration (number of hours) of contract o, and $\breve{R}_{t\omega}$ the actual solar radiation at hour t and scenario ω.

$$R_\omega = \frac{1}{D} \sum_{t \in \mathbb{D}} \breve{R}_{t\omega} \tag{2}$$

Constraints (1d) and (1e) ensure that z_ω quantifies the distance between ξ and each profit scenario Π_ω, for only those scenarios below ξ (VaR at the optimum), which are required to compute the CVaR.

3.2. *Technical operation constraints*

The general technical operation scheme considered is shown in Figure 2 and recast within constraints (1f)-(1r).

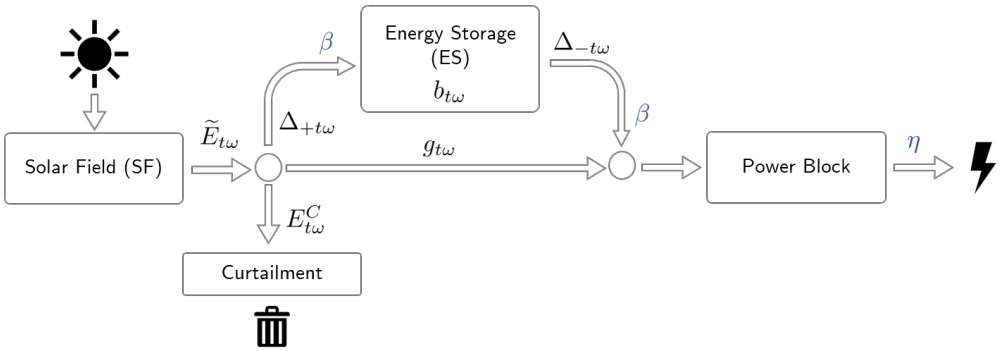

Figure 2.: Basic functioning of a solar-based power plant with storage.

For CSPs, the power collected by the Solar Field (SF) and stored in the Energy Storage (ES) is thermal power, so the power block represents the conversion of heat into electricity through a turbine with the associated efficiency η. On the contrary, PVs directly generate electricity in the solar field (solar panes), which can be stored in the battery or directly sent to the main grid. In this case, the power block and its efficiency η can characterize the conversion process between DC and AC currents through an inverter.

The maximum amount of electricity that can be traded in the spot market is defined in (1f) including the power from the SF, $g_{t\omega}$, plus the net power discharged from the storage, $\beta\Delta_{-t\omega}$, multiplied by the efficiency η, minus the energy traded in the futures market. Note that the ES is modeled with a charge and discharge loss efficiency of β. Constraint (1h) imposes a lower bound on futures trading quantity q^F, as we allow short positions in the futures market, at a given time t, up to the lowest realization of $q^S_{t\omega}$ for all scenarios ω. Equation (1i) establishes that the power generated by the SF, i.e., the exogenous random parameter $\widetilde{E}_{t\omega}$, matches the power directly sent to the grid $g_{t\omega}$ plus the energy redirected to charge the ES ($\Delta_{+t\omega}$) and the power curtailed $E^C_{t\omega}$, for every time t and scenario ω. In particular, the power curtailed $E^C_{t\omega}$ allows balancing those operating periods and scenarios where there is a need to discard part of the energy generated by the SF, i.e., is not profitable to send further energy to the grid and the ES is already at its full capacity. Moreover, $\widetilde{E}_{t\omega}$ is proportional to the surface of the solar field h (e.g., the heliostat reflective area for CSPs or the surface covered by panels for PVs) and the solar radiation according to equation (3).

$$\widetilde{E}_{t\omega} = h\breve{R}_{t\omega} \qquad \forall t \in \mathbb{D}, \omega \tag{3}$$

Equations (1j) and (1k) describe the dynamics of the energy available in the ES, $b_{t\omega}$, within the considered periods. It is computed as the energy available in the ES at the previous period, $b_{t-1,\omega}$, plus the charge, $\eta\Delta_{+t\omega}$, minus the discharge, $\Delta_{-t\omega}$, at period t and scenario ω. To ensure that the total energy discharged and charged are equal within the time horizon considered, we impose in (1k) that the status of the ES at times $t = T$ and $t = 0$ needs to be the same. Upper and lower capacity bounds for the energy available in the ES, as well as its maximum charging and discharging

capacities, are imposed by (1l), (1m), and (1n), respectively. Subscript "a"stands for either "$a = +$" (storage charging) or "$a = -$" (storage discharging). Constraint (1o) sets $\bar{q}$ as the maximum amount of electricity that the plant can generate. Finally, constraints (1p)-(1r) impose the non-negativity on some of the variables.

3.3. *Characteristics of the Financial Options*

Forward trading is the first financial instrument to manage risk, as the generator may decide to sell ahead an energy quantity of q^F. The advantage of such action is that the revenue is no longer dependent on price fluctuations in the spot market ahead of generation. We are following the literature on the relationship between spot and forward prices (e.g., Bodie et al. 2014, Ch.22), and we assume that the futures price is such that the non-arbitrage pricing rule holds. The forward price equals the discounted risk-neutral expected spot prices, as summarized in equation (4):

$$F = \frac{\rho^d}{D} \sum_{t \in \mathbb{D}} \sum_{\omega} \frac{S_{t\omega}}{\Omega} \tag{4}$$

This is a weaker form of the non-arbitrage argument that does not require the underlying asset to be stored. It holds for services and betting as well. In this sense, the non-arbitrage argument just says there is no investment portfolio with an expected profit. Note that if $F < \frac{\rho^d}{D} \sum_{t \in \mathbb{D}} \sum_{\omega} \frac{S_{t\omega}}{\Omega}$ or $F > \frac{\rho^d}{D} \sum_{t \in \mathbb{D}} \sum_{\omega} \frac{S_{t\omega}}{\Omega}$ then F would tend to increase, or decrease, respectively so that the non-arbitrage argument holds.

This is different from the strong non-arbitrage argument (e.g., Hull 1993, Ch.3), which states that (at any given time t) there is a relationship between the spot and futures prices at time t: this relationship is based on the argument that the underlying asset would be purchased and stored for the time of the contract (we do not impose this condition).

Other components of the profit function (1b) and (1c) are the costs and revenues from investing in option contracts. The model considers two types of financial options (a call and a put), whose value depends on the average solar radiation during the delivery period, $R_{o\omega}$, and on the respective exercise of solar radiation R_o, which is the threshold that determines whether the option is in the money or not.

The premiums, i.e., the prices paid by the call and put options, are calculated by (5), which assumes the non-arbitrage condition: the price is determined by risk-neutral agents, and it is equal to the discounted present value of the expected revenues, i.e., the pricing of these weather derivatives follows the same non-arbitrage argument used for financial options (Bodie et al. 2014, Ch.21).

$$c_o = \frac{\rho^d}{\Omega} \sum_{\omega} \sigma_o \left(R_\omega - R_o\right)^+ \tag{5a}$$

$$p_o = \frac{\rho^d}{\Omega} \sum_{\omega} \sigma_o \left(R_o - R_\omega\right)^+ \tag{5b}$$

The *call option* gives the owner the right to purchase electricity if the solar radiation is higher than R_o. The *put option* gives the owner the right to sell electricity if solar radiation is less than R_o. Both options can be bought and sold for a pre-determined period of the day ($\mathbb{D}$). The option premiums for the call (c_o) and the put (p_o) represent

how much the company pays to buy (receives from selling) a call and a put option, respectively, when the company buys (sells) a call $q_o^c > 0$ ($q_o^c < 0$) or a put $q_o^p > 0$ ($q_o^p < 0$). Therefore, from equation (1b), it then follows that the cost of purchasing (revenue received from selling) options is equal to $\sum_{o\in\mathbb{O}} (q_o^c c_o + q_o^p p_o)$.

The value of these options on solar radiation depends on the difference between the average radiation on the day when the option contract can be exercised (R_ω) and the exercise solar radiation R_o, which stands for the reference radiation on which the contract is based), standardized by the tick size σ_o converting radiation into monetary units. The value of the call options purchased or sold by the company is equal to $\sum_{o\in\mathbb{O}} q_o^c \sigma_o (R_\omega - R_o)^+$. When the average radiation exceeds the exercise radiation, the call option is exercised and is valuable. For this reason, the call option buyer makes a profit when there is more solar radiation than expected. If it is below expectation, the call has no value, and the seller (buyer) keeps (loses) the premiums collected (paid).

The value of the put options is equal to $\sum_{o\in\mathbb{O}} q_o^p \sigma_o (R_o - R_\omega)^+$. When the average radiation is *less than* the exercise radiation, the put options are valuable and are exercised by the buyer. The buyer of the put option makes a profit when radiation is less than expected, and the seller makes a profit (the collected premiums) when radiation exceeds the exercise radiation.

4. Analysis of the Main Properties of the Model

All the proofs of the results presented in this section are in the Online Appendix C. We start the analysis by considering how the CVaR affects the generator's decisions; Lemma 4.1 describes how the CVaR restricts the scenarios included in the objective function to those with the α-lowest profits, and each scenario is included with the same probability.

Lemma 4.1. *The λ_ω represents the probability distribution over the states in the tail of the profit function, such that: a) If $z_\omega > 0$, then $\lambda_\omega = \frac{1}{\alpha\Omega}$ and $\Phi_\omega^Z = 0$; b) When $z_\omega = 0$ and $\xi = \Pi_\omega$ then $\lambda_\omega \leq \frac{1}{\alpha\Omega}$ and $\Phi_\omega^Z \leq \frac{1}{\alpha\Omega}$.*

Lemma 4.1 is a critical insight as it shows the λ_ω can then be used to calculate a risk-adjusted expected profit function, i.e., the CVaR, allowing a reformulation of the problem in a more analytical tractable format.

Let ω^z be the scenarios in the tail of the profit function. We proceed by analyzing the basic properties of the options on solar radiation, as summarized in Lemma 4.2, which proves that the risk-averse expectation over the tail radiation of the options is a direct function of the percentage α.

Lemma 4.2. *The risk-averse expected radiation above (below) the exercise threshold is a proportion α of the respective risk-neutral expectation: for the call option $\sum_{\omega^z} (R_{\omega^z} - R_o)^+ = \alpha \sum_\omega (R_\omega - R_o)^+$, and for the put option $\sum_{\omega^z} (R_o - R_{\omega^z})^+ = \alpha \sum_\omega (R_o - R_\omega)^+$.*

Lemma 4.2 is important for three reasons. First, it shows an interaction between the choice of option contracts and the degree of risk aversion, determining the scenarios a risk-averse generator considers when choosing the best generation and trading strategy. Second, it proves that the lower the degree of risk aversion (i.e., the higher the α), the higher the optimism in regards to the amount of radiation above (call option) or below (put option) the threshold. Third, it proves that these options contracts are used to

manage quantity risk as the optimal policy consists of choosing which scenarios (with higher or lower radiation) to include in calculating the conditional expectation.

Let ω^+ (ω^-) stand for the subset of scenarios in which the call (put) is valuable. Proposition 4.3 analyzes how solar radiation affects the relationship between call and put solar radiation prices. For a given exercise radiation level R_o, the higher the total radiation above the threshold ($\sum_{\omega^+} R_{o\omega^+}$) and the lower the level of radiation below the threshold ($\sum_{\omega^-} R_{o\omega^-}$), the higher the value of the call and the lower the level of the put.

Proposition 4.3. *The call price is equal or greater than the put price if and only if* $\sum_{\omega^+} R_{o\omega^+} \geq \sum_{\omega^-} R_{o\omega^-}$.

The analysis now focuses on the relationship between spot and forward trading. More specifically, during daylight hours ($t \in \mathbb{D}$), as proved in Proposition 4.4, a risk-averse generator expects to *buy* electricity in the spot market if and only if the expected generation is less than sales in the forward market. This strategy is profitable when the price received for selling forward is higher than the present value of the expected spot price at hour t.

Proposition 4.4. *At hour* $t \in \mathbb{D}$, $\frac{1}{\Omega}\sum_{\omega} q^S_{t\omega} < 0$ *if and only if* $q^F > \frac{\eta}{\Omega}\sum_{\omega}(g_{t\omega} + \beta\Delta_{-t\omega})$.

However, it is not clear from Proposition 4.4 if storage affects the number of hours the generator expects to *buy* in the spot market as the additional generation available can be both allocated to be sold in the spot or meet the obligations to the futures market. Therefore, it is interesting to understand under which conditions it leads to higher purchases in the spot market, sales in the forward market, or both.

We investigate this issue in Proposition 4.5, which follows that the quantity sold in the forward market, q^F, equals the expected production in the day minus the expected sales in the spot market. For this reason, a production system equipped with storage can increase average output and, consequently, boost trade in the spot market.

Proposition 4.5. *Let* ω^z *stand for the tail scenarios considered by the risk-averse generator, then* $q^F = \frac{\eta}{D\alpha\Omega}\sum_{t\in\mathbb{D},\omega^z}(g_{t\omega^z} + \beta\Delta_{-t\omega^z}) - \frac{1}{D\alpha\Omega}\sum_{t\in\mathbb{D},\omega^z} q^S_{t\omega^z}$ *and therefore a generator owning storage sells more in the futures market.*

We further try to understand how risk aversion affects storage and futures trading utilization. Let q^F_1 and q^F_0 stand for the sales in the forward market with and without storage, respectively. As proved by Proposition 4.6, the higher the degree of risk aversion (i.e., the lower the α), the higher the difference between the sales in the futures market with and without storage. Hence, as the degree of risk aversion increases (α converges to 0), the futures market sales also increase. This is a significant result, as it shows that storage management depends on the managerial attitudes towards risk. There is a higher capacity commitment when management is risk averse.

Proposition 4.6. *Let* ω^z *stand for the tail scenarios considered by the risk-averse generator, everything else constant, the impact of storage on forward trading is equal to* $q^F_1 - q^F_0 = \frac{\eta}{D\alpha\Omega}\sum_{t\in\mathbb{D},\omega^z}\beta\Delta_{-t\omega^z}$.

Furthermore, this result can be extended to consider the impact of storage and risk aversion on optimal spot trading. Proposition 4.7 shows that storage increases spot trading for a given q^F, regardless of the degree of risk aversion.

Proposition 4.7. *At daylight hour $t \in \mathbb{D}$, $q^S_{t\omega} = \eta\,(g_{t\omega} + \beta\Delta_{-t\omega}) - q^F$, then for a given q^F, the higher the $\Delta_{-t\omega}$ the higher the $q^S_{t\omega}$.*

It follows from identities (2) and (3), $R_\omega = \frac{1}{D}\sum_{t\in\mathbb{D}} \breve{R}_{t\omega}$ and $\widetilde{E}_{t\omega} = h\breve{R}_{t\omega}$, that in hours with higher radiation there is a higher production capacity. Proposition 4.8 and Proposition 4.9 extend this trivial observation to analyze the relationship between option prices and solar radiation. Proposition 4.8 proves that the higher the total radiation in a day $\sum_{t\in\mathbb{D}} \widetilde{E}_{t\omega}$, the higher the value of the call options and the lower the value of put options. Consequently, we expect higher call prices in the summer and higher put prices in the winter.

Proposition 4.8. $c_o = \frac{\rho^d}{\Omega}\sigma_o \sum_\omega \left(\frac{1}{hD}\sum_{t\in\mathbb{D}} \widetilde{E}_{t\omega} - R_o\right)^+$ *and* $p_o = \frac{\rho^d}{\Omega}\sigma_o \sum_\omega \left(R_o - \frac{1}{hD}\sum_{t\in\mathbb{D}} \widetilde{E}_{t\omega}\right)^+$.

Furthermore, Proposition 4.9 extends this analysis by establishing a relationship between electricity generation and storage with option prices. More specifically, it is proven that a) the higher the call prices, the higher the electricity generation and storage, and b) the higher the put options, the lower the electricity generation and production.

Proposition 4.9. *In the optimal policy, $\frac{\rho^d\sigma_o}{hD\Omega}\sum_{\omega^+}\sum_{t\in\mathbb{D}}(g_{t\omega} + \Delta_{+t\omega}) = c_o + \alpha\rho^d\sigma_o R_o$ and $\frac{\rho^d\sigma_o}{hD\Omega}\sum_{\omega^-}\sum_{t\in\mathbb{D}}(g_{t\omega} + \Delta_{+t\omega}) = \alpha\rho^d\sigma_o R_o - p_o$.*

Finally, Proposition 4.10 proves that the risk-adjusted expected profit from options trading is zero, proving that the results of the model are consistent with the non-arbitrage pricing assumption of financial theory, even after considering storage and the radiation option.

Proposition 4.10. $\mathbb{E}(\Pi_o^{t\in\mathbb{D}}) = 0$.

5. Case Study

In this case study, we evaluate and compare the operation of a CSP and a PV plant in southern Spain. Table 1 summarizes the specific parameters defining the problem for each type of technology. Each simulation includes $\Omega = 10000$ scenarios. The proportion of observations in the tail of the profit distribution represents risk aversion. In the base case, it is set to $\alpha = 0.05$. The technical details of the considered CSP and PV plants have been based on Domínguez et al. (2012) and DiOrio et al. (2020), respectively.

For the CSP plant, the electricity generation cost $k_{t\omega}$ is considered fixed to 0.1 €/MWh for all time t periods and scenario ω. The CSP conversion efficiency from thermal power to electricity (p.u.) is $\eta = 0.38$. The CSP loss efficiency of thermal storage (p.u.) is $\beta = 0.95$. The minimum energy content of the TES is $\underline{b} = 45$ MWh-t; and the maximum energy content of the TES is $\bar{b} = 700$ MWh-t. The maximum electric power output is $\bar{q} = 50$ MW-e. The maximum thermal power transferred to (taken from) the TES is $\Delta = 50$ MW-e/h. The hourly solar radiation $\breve{R}_{tw}$ is transformed into thermal power $\widetilde{E}_{t\omega}$ according to (3), and by assuming an upper bound of $E^{max} = 150$MWh-t, where $h = 500000$ m^2 is the total heliostat reflective area considered. For the PV plant, the values for the equivalent parameters can also be checked, if different, in Table 1 between parenthesis. In this case, all the power

Table 1.: Problem Parameters

$\alpha = 0.05$: Proportion of observations on the tail of the profit distribution.
$\sigma_o = 2.5 \times 10^5$: Tick size, i.e., monetary unities per radiation unit.
$\eta = 0.38$ (= 0.976): CSP (PV) conversion efficiency from thermal power (DC) to AC electricity (p.u.).
$\beta = 0.95$ (= 0.982): CSP (PV) loss efficiency of thermal (battery) storage (p.u.).
$\rho^d = 0.99$: discount factor.
$d = 90$ Number of days from the present to the date of delivery of the contract.
$k_{t\omega} = 0.1$ (= 0.1) €/MWh: CSP (PV) generation cost at time t and scenario ω.
$E^{max} = 150$ MWh-t (= 150 MWh-e): Maximum amount of thermal power (electrical power) that CSP (PV) can capture in a given hour.
$\widetilde{E}_{t\omega}$: MWh-t: Thermal (Electrical) power captured by CSP (PV), at time t, and scenario ω (Section 5.1).
$\underline{b} = 45$ MWh-t (= 15 MWh-e): Minimum energy content of CSP TES (PV battery).
$\overline{b} = 700$ MWh-t (= 150) MWh-e: Maximum energy content of CSP TES (PV battery).
$\bar{q} = 50$ (= 115.38) MW-e: Maximum electric power output CSP (PV).
$\Delta = 50$ (= 37.5) MW-e/h: Maximum thermal power transferred to/taken from CSP TES (PV battery)
$S_{t\omega}$ €/MWh: spot price at time t and scenario ω (Section 5.1).
F €/MWh: futures price (Section 5.1).
c_o: call option premium (Section 5.1).
p_o: put option premium (Section 5.1).
R_ω: average radiation for scenario ω (Section 5.1).
R_o: exercise radiation for option o (Section 5.1).
$\Omega = 10000$: number of scenarios.

is directly generated and transferred as electricity so that the conversion efficiencies represent the DC to AC conversion process.

The parameters associated with the weather options are: $\sigma_o = 2.5 \times 10^5$ is the tick size, i.e., monetary unities per radiation unit; the discount factor $\rho = 0.99$; the number of days from the present to the date of delivery of the contract is $d = 90$. The considered daylight hours $t \in \mathbb{D}$, where the future and option contracts are active, are defined from 7:00 to 21:00 (included).

5.1. *Spot Prices and Solar Energy*

Figure 3 illustrates a subset of the hourly spot price scenarios and their mean values, considered for the representative days of summer and winter. To generate these scenarios, we have first collected all hourly prices within January (winter case) and July 2019 (summer case) from ESIOS (2022). Then, we have estimated their corresponding hourly mean and covariance, which are used to generate $\Omega = 10000$ random realizations of a 24-multivariate normal distribution, i.e., each scenario corresponds to a particular 24-hour price trajectory. Both sets of prices are time-dependent, i.e., are a function of the hour of the day. Most importantly, the summer prices in Figure 3a are much less volatile than the winter prices in Figure 3b, which suggests that the strategies for risk hedging are possibly more important in the winter than in summer days. The futures price F is computed as the average of the spot prices during the contract duration (4).

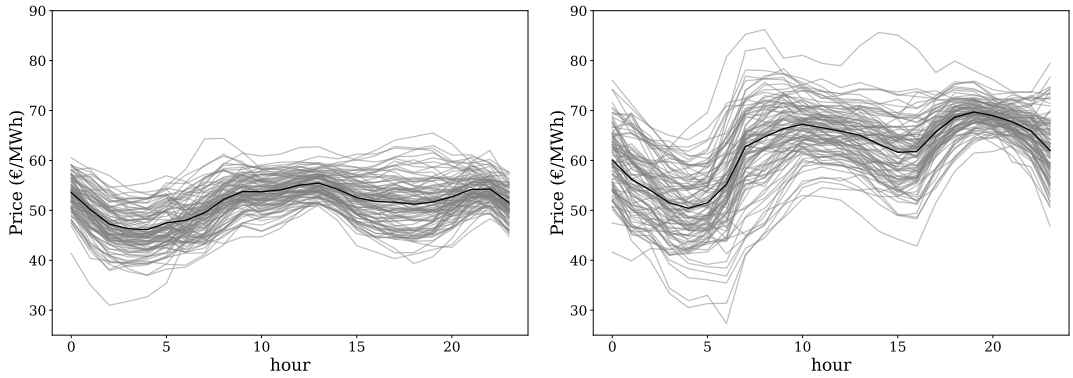

(a) Summer. (b) Winter.

Figure 3.: Spot prices.

To generate scenarios for SF thermal production ($\widetilde{E}_{t\omega}$), we have considered hourly radiation data for a specific location in Spain, Extremadura Region (39°13'45.7"N 5°23'52.4"W) for January (winter case) and July 2019 (summer case), which can be downloaded from the ERA5-Land dataset ECMWF Copernicus project (2022). In particular, we have analyzed the variable "surface net solar radiation" [J m^{-2}]. These hourly data are then translated into $\Omega = 10000$ scenarios by following a similar normal multivariate approximation, which is later converted into scenarios of $\widetilde{E}_{t\omega}$ production (MWh-t) according to the CSP and PV technical characteristics described in the previous section, and by using E^{max} as an upper bound for every time t and scenario ω.

Figure 4 represents a subset of the scenarios and their hourly mean for the solar field production capacity on days of summer (Figure 4a) and winter (Figure 4b). The first obvious observation is that solar production is concentrated in a smaller set of hours in the winter, and the average output at the peak times is lower in the winter. Second, and more interesting, is the increased volatility of solar production in the winter.

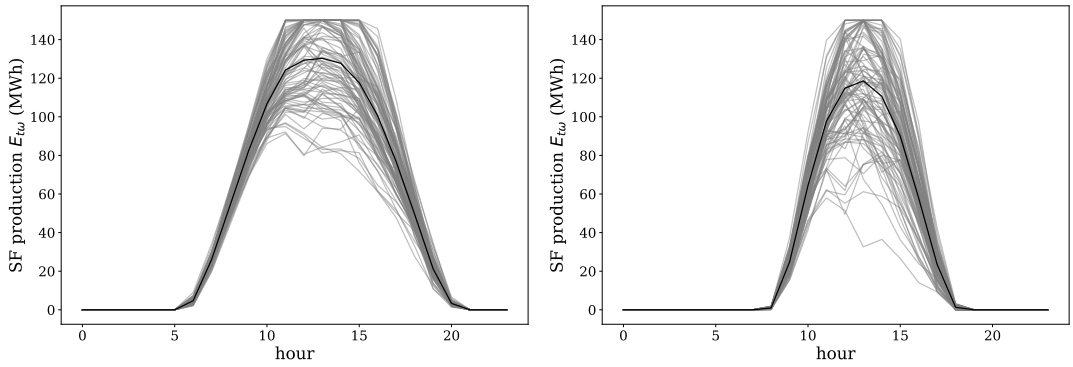

(a) Summer. (b) Winter.

Figure 4.: SF production.

Therefore, Figures 3 and 4 show that the solar plant is subject to higher price and production risk during winter. If the futures market can be used to address the price hedging problem, the producer needs another instrument to handle the quantity risk: the weather options. The average and exercise radiation (R_ω and R_0) and the call and put optimum premiums (c_o and p_o) are computed from the radiation time series

according to expressions (2), (5a) and (5b).

The summer and winter months (January and July) characterize two very different price and solar radiation patterns. We explore their potential impact on the trading of forward contracts and financial options. Moreover, the large number of scenarios generated for each month provides a detailed representation of the profit distributions, which, combined with a CVaR optimization, aim to capture long-term potential risks (price and quantity) of renewable production.

5.2. *TES Operations and Spot Trading*

We start the analysis of Figure 5 by studying the operation of the solar power plants and how these are related to spot trading. Figures 5a) and 5c) depict the expected spot trade and the operation of the CSP plant in the summer and winter, respectively. As expected, the number of hours the plant sells in the spot market is higher in summer (peak sales and number of hours). However, purchasing from the spot market is narrower but more profound in the summer.

The operations of the PV plant are very similar to the behavior described for the CSP, as seen in Figures 5b) and 5d). The major difference is the level of generation and purchases from the spot market (which are higher in the PV) and the relative importance of the storage system, which is higher in the CSP.

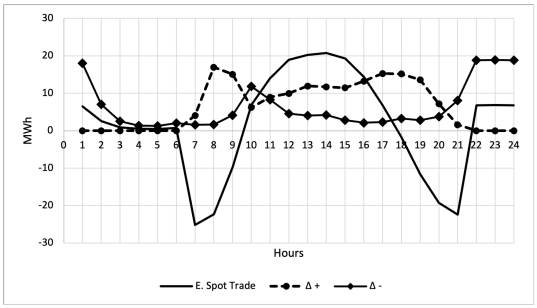

(a) CSP Summer: Operations and Spot Trading.

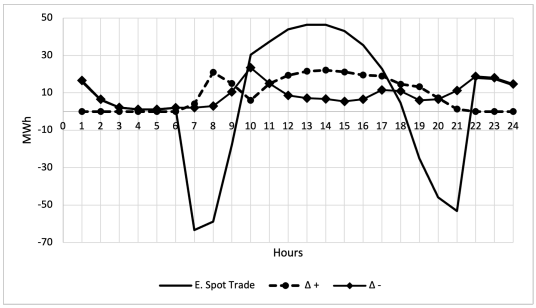

(b) PV Summer: Operations and Spot Trading.

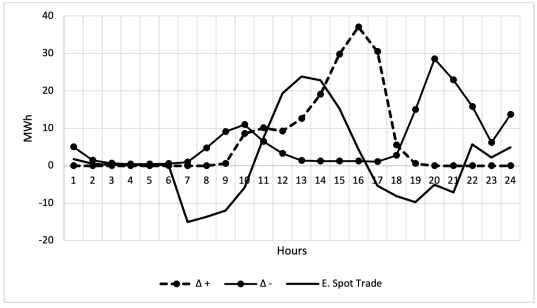

(c) CSP Winter: Operations and Spot Trading.

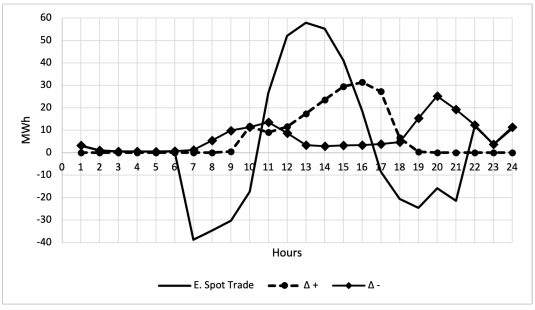

(d) PV Winter: Operations and Spot Trading.

Figure 5.: Operations of CSP and PV in Summer and Winter.

The first interesting observation is that the plants sell energy in the spot market *during the night*, both in the summer and winter. The operation of the storage systems is highly non-linear. Surprisingly, the storage systems are discharged even during the day while simultaneously charged. (Note that as these systems generally do not allow simultaneous charging and discharging, what is happening is that in some scenarios,

there is charging, and in others, there is discharging. As the Figure reports, the mean values are both positive.) Moreover, the charging of the storage system depends on electricity demand and not only on the availability of solar energy. In the summer, the storage systems are charged early in the morning when radiation is weak: the plants buy electricity from the spot market. When demand decreases, the plant repurchases energy from the spot market in the evening.

Surprisingly, in the summer, the plants store energy while at the same time buying electricity in the spot market. In the winter, on the other hand, the storage systems are charged when the plants are also selling in the spot market and discharged almost entirely early at night because, on average, prices are higher at night, see Figure 3b).

Next, Figure 6 shows that, in this case, the degree of risk aversion does not significantly affect the level of electricity bought and sold in the spot market at any given season. Instead, it is mostly affected by the technology (higher trading with PV) and the storage device (higher when no device exists). The CSP plant trades higher volumes in the spot market in the winter. The result is mixed for the PV plant.

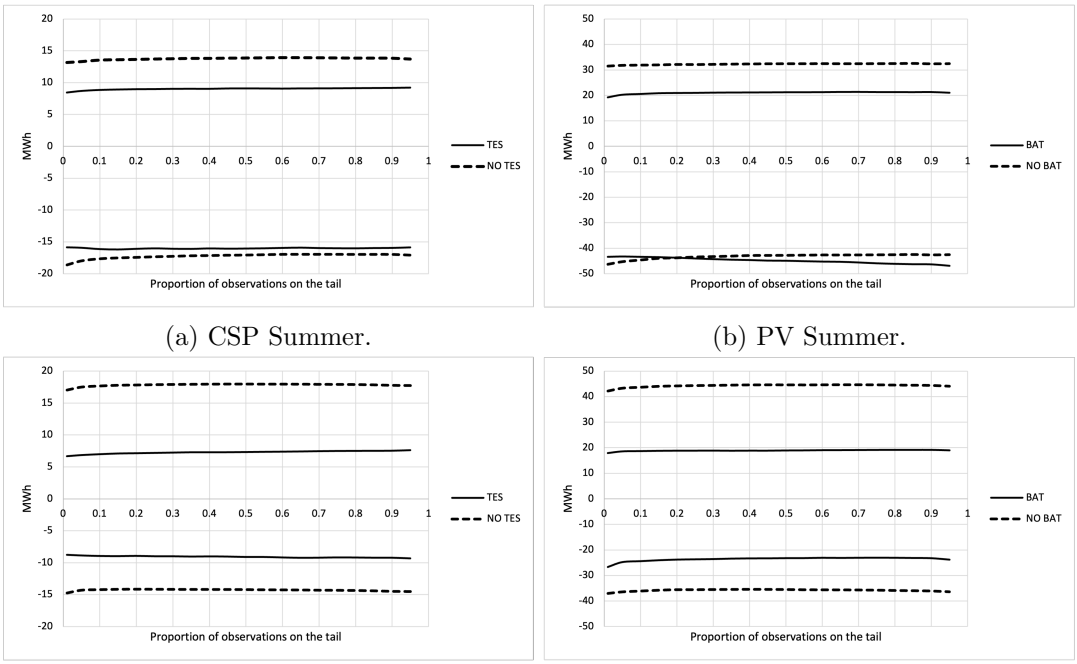

(a) CSP Summer. (b) PV Summer.

(c) CSP Winter. (d) PV Winter.

Figure 6.: Sensitivity analysis of spot trading to the proportion of observations on the tail.

5.3. *Futures Trading*

Figure 7 depicts the spot and futures trading results in both summer and winter for the CSP and the PV plants. (Note that for each optimal q^F, there are multiple possible realizations (dots) for each level of risk aversion because each dot corresponds to a different exercise radiation level R_0.)

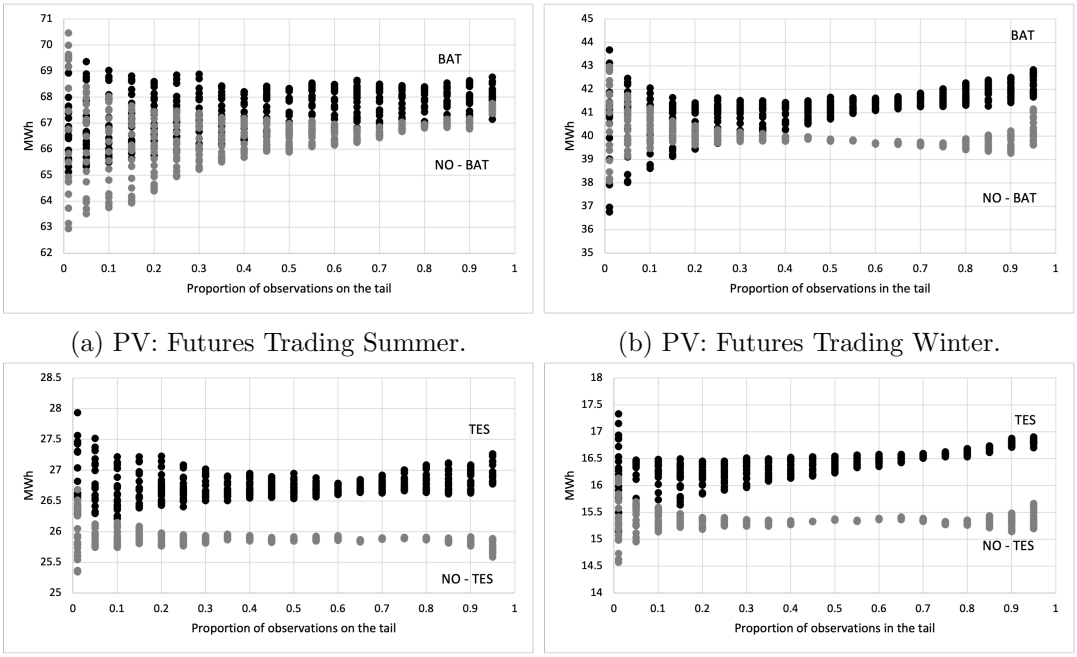

(a) PV: Futures Trading Summer.

(b) PV: Futures Trading Winter.

(c) CSP: Futures Trading Summer.

(d) CSP: Futures Trading Winter.

Figure 7.: Futures Trading.

Figures 7a and 7b summarize the futures trading for the PV plant, comparing the optimal policy with (BAT) and without battery (NO-BAT) in the Summer and Winter, respectively. First, in the Summer, the impact of the battery on futures trading is minimal and not statistically significant. Risk aversion had a considerable effect on the optimal trading strategy: the lower the degree of risk aversion (the proportion of observations on the tail is closer to 1), the higher the futures trading, especially when there is no battery. Second, there is a decreased reliance on the futures market in the winter. There is a significant difference between future sales and whether there is a battery. When the degree of risk aversion decreases (proportion on the tail above 0.5), when there is a battery, the sales in the futures market increase more than with no battery. In this case, the battery plays a vital role in shaping the generator's trading strategies: the battery provides a degree of safety regarding available generation, allowing the generator to sell in the futures market with a lower risk of failing to meet demand.

Similarly, for the CSP, Figures 7c and 7d describe the futures trading with (TES) and without (NO-TES) thermal storage in summer and winter days, respectively. First, both in the Summer and Winter, futures trading is higher with the TES (in line with Proposition 4.5). Second, unsurprisingly, the CSP sells more in the futures market in the summer, as it has a higher production potential. Third, when there is a TES, the lower the degree of risk aversion (i.e., when the proportion on the profit tail approaches 1), the higher the sales in the futures market; this is because the TES can be used to meet the commitments to the futures market when electricity production from solar energy is less than expected. Fourth, the risk-averse producer's futures trading volatility is significantly higher (lower proportion on the tail).

5.4. *Option Trading*

The option prices are depicted in Figure 8 as a function of the exercise solar radiation in summer (Figure 8a) and in winter (Figure 8b) days. The options are priced for radiation levels ranging from 5% to 95% (from about 58 to 91 in the summer and 31 to 61 in the winter).

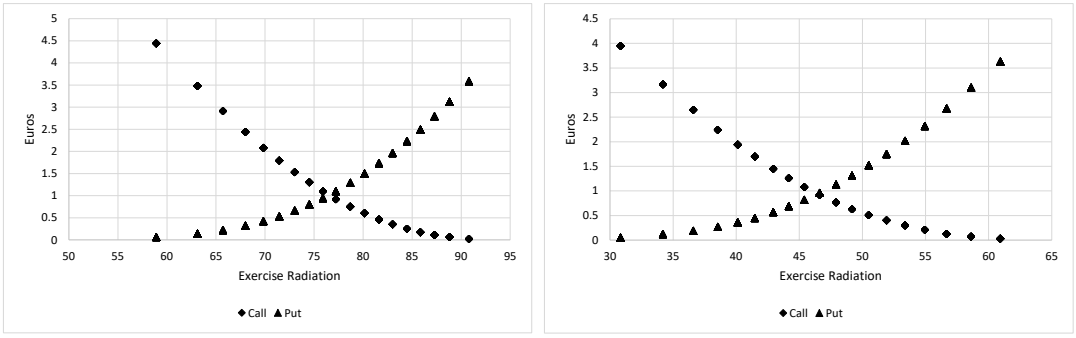

(a) Summer. (b) Winter.

Figure 8.: Options Prices.

The option prices range from 0 to about 5 euros per contract. The higher the exercise radiation: a), the higher the put price, as the probability that the radiation on a given day exceeds the exercise values decreases and, therefore, it is more likely that the put option is in the money on the day of delivery; b) likewise, the lower the call price, as the probability that the option is in the money decreases with the increase in the exercise radiation. The values of the two options cross at 1 euro per contract, both in the summer and winter. In line with Proposition 4.3, the exercise radiation at which call and put prices are equal is higher in the summer. Moreover, as proved in Proposition 4.8, for the same exercise radiation, the call prices are higher in the summer and put prices higher in the winter.

Next, we analyze options trading in summer (Figure 9) and winter (Figure 10). The first surprising result in all simulations, both in the Summer and Winter, is that the optimal strategy is always to *sell calls and buy puts*. This is particularly unexpected as with this trading strategy; the solar plant is maximizing both potential risks and returns from options trading: a) when the radiation is above average, the solar plant loses the premium paid by the put options and has losses in the sold calls as well; b) when the radiation is below average, the plant profits from the bought puts and would keep the premiums of the calls sold that would be out-the-money. In summary, the plant is betting that the radiation is below average, as it could sell the electricity stored at a higher price and profit from options trading. Nonetheless, even though this trading strategy is highly speculative, the expected profit from the options trading is zero because the options are priced so that the respective premiums equal the expected discounted revenues.

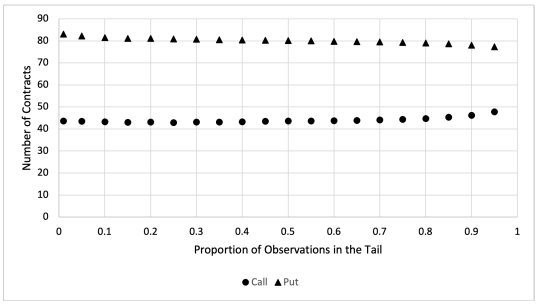

(a) CSP: NO TES.

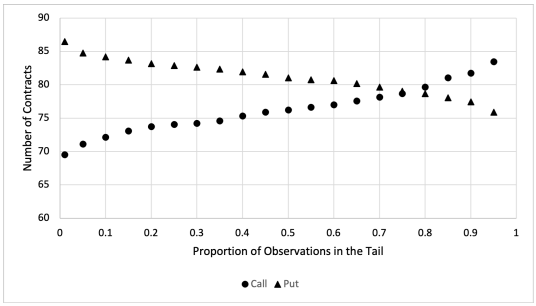

(b) CSP: TES.

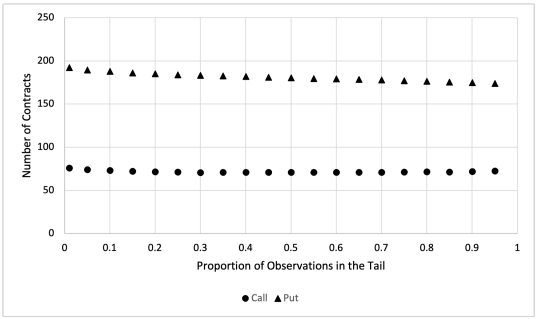

(c) PV: NO Battery.

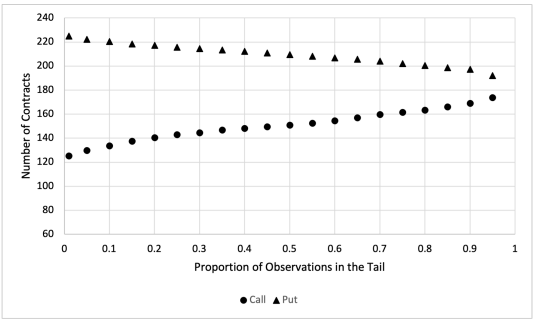

(d) PV: Battery.

Figure 9.: Number of Option Contracts Traded in the Summer as a Function of Risk Aversion.

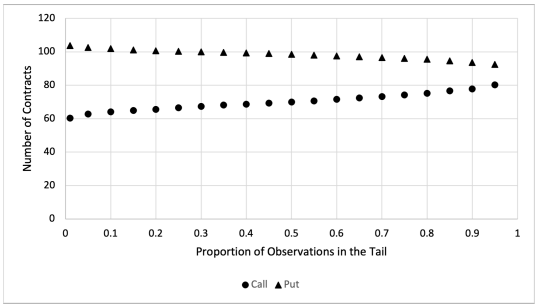

(a) CSP: NO TES.

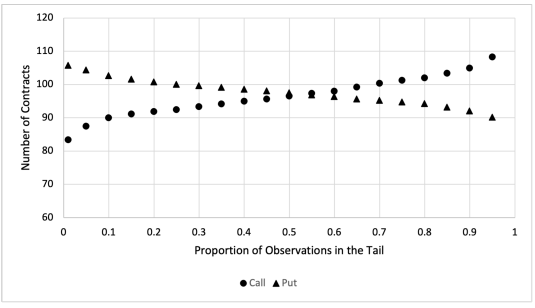

(b) CSP: TES.

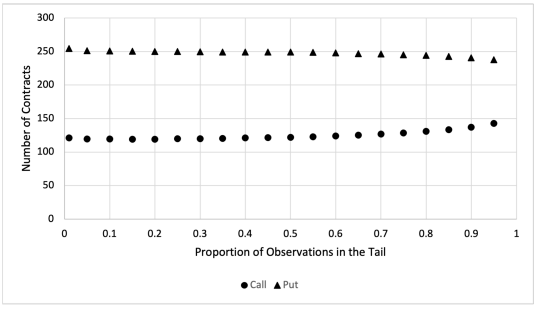

(c) PV: NO Battery.

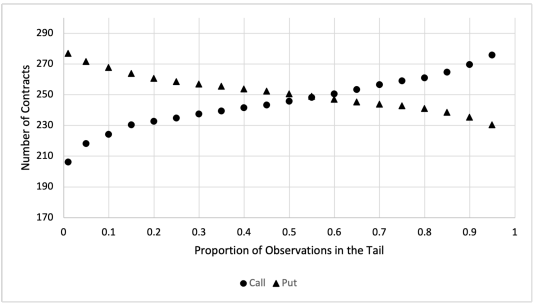

(d) PV: Battery.

Figure 10.: Number of Option Contracts Traded in the Winter as a Function of Risk Aversion

.

The results in Figures 9 and 10 can be analyzed from three essential perspectives: the impact of weather (Summer and Winter), risk aversion, and storage system ownership

on the optimal option trading strategies, as the figures summarize the number of contracts as a function of the proportions of observations on the tail, without and with the storage system. First, it is surprising to observe the impact of risk aversion on using options. The CSP and the PV with a storage system sell significantly more call options, and the numbers increase as the degree of risk aversion approaches neutrality. As the expected value of the options is zero, the evidence suggests that as risk aversion increases (i.e., the proportion on the tail approaches zero), the plant sells fewer options, reducing the risk associated with higher radiation levels. Second, for both CSP and PV generators, the higher the risk aversion, the higher the number of put contracts purchased. This suggests an interaction between the storage system and risk aversion and purchasing put and selling call options that define the optimal risk management strategy. With a storage system, a risk-averse plant decreases risk by purchasing put options that are out of the money on high radiation days. It profits from increased sales at night due to increased storage levels and lower purchases in the spot market.

In Winter, when radiation is lower, both the CSP and the PV generators sell many more call options than in the Summer (compare Figures 9 and 10). This aligns with our analysis of electricity prices and radiation levels as the plant is exposed to higher price and generation risks in winter, hence the increased options trading. Additionally, in Winter, as summarized in Figure 10, storage ownership strongly influences the risk management strategy, as the plants sell more call options, specifically if it is risk-neutral.

5.5. *Profit and CVaR*

We proceed by studying how profits (Figures 11), VaR, and CVaR (Figures 12) are affected by the season, storage system, and degree of risk aversion.

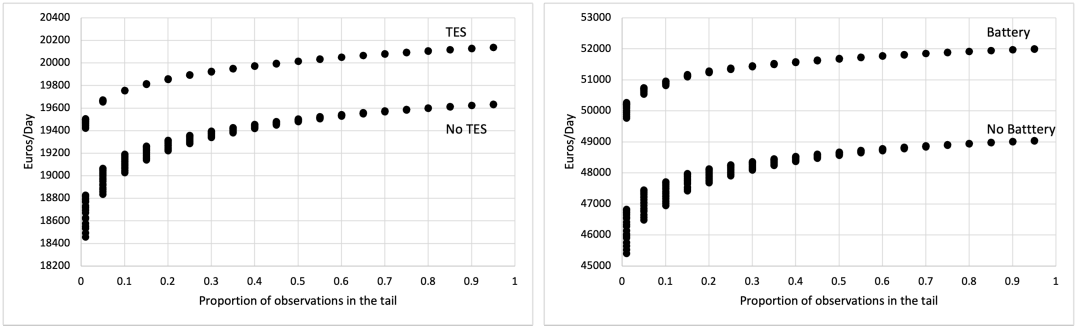

(a) CSP. (b) PV.

Figure 11.: Profit as a Function of the Level of Risk Aversion.

First, the storage systems create value for the plants. How much depends on the degree of risk aversion, season, and storage system. For a CSP plant, if risk neutral, the TES makes about 728 euros/day (representing an increase of 3.8% in profitability); if risk averse, the TES makes 890 euros/day (representing an increase of 4.8% in profitability). For a PV plant, if risk neutral, the battery makes about 2960 euros/day (representing an increase of 6.0% in profitability); if risk averse, the TES makes 3795 euros/day (representing an increase of 8.3% in profitability).

Finally, Figure 12 describes the VaR and CVaR for the CSP and PV plants, with and without storage systems. The VaR and CVaR are higher for the risk-neutral power plants, as is the difference between VaR and CVaR. The importance of the storage

systems is evident in the volatility of VaR and CVaR for each level of risk aversion: when risk aversion is high, if there is no storage system, exercise radiation is essential in determining the level of the risk measures (as each point in the series, for any given proportion in the tail), corresponds to a different solar radiation level.

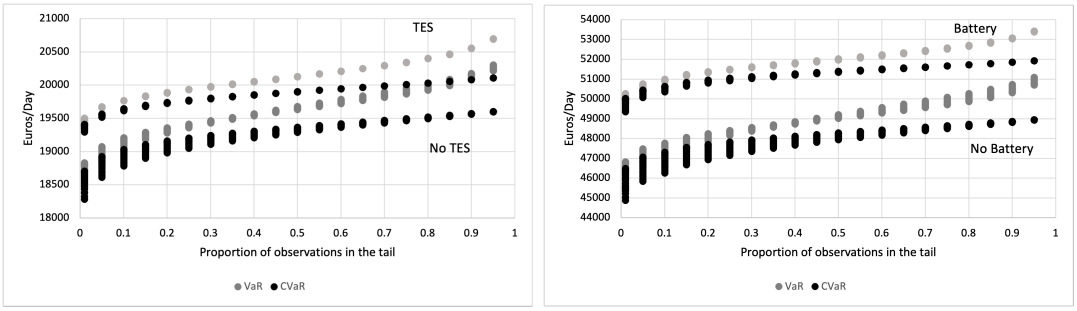

(a) CSP. (b) PV.

Figure 12.: CVaR.

6. Conclusions

The EU aims to be climate-neutral by 2050 (EC Climate Action 2022). A central component of this plan is the investment in renewable electricity, such as CSP and PV power plants, which allow the electricity network to maintain quality and sustainability. However, high levels of renewable penetration can decrease system reliability unless these plants are complemented with storage capabilities.

A drawback of these renewable technologies is that, despite the new storage technologies, their profitability is still very dependent on the existence of effective financial instruments, as they face high levels of uncertainty (including market outcomes and renewable resource availability, i.e., quantity risk). For this reason, in this article, we study solar radiation-based derivatives, which link weather conditions with power plant energy production, and we study their important implications for risk management.

To this end, we have analyzed the operation of these CSP and PV plants in combination with storage, modeling their typical production patterns on winter and summer days, as they depend on solar radiation levels. We employ a large two-stage stochastic programming problem, where the first-stage models the trading in the futures markets (physical) and through weather options (financial), and the second-stage represents the scenario-dependent spot market trading and the operation of the power plant. Moreover, we account for risk aversion, including the plant's profit CVaR in the objective function. This innovative analysis considers how the optimal production of CSPs and PVs depends on spot and future prices, the ability to store energy, weather derivatives, and the managerial risk profile.

Our central managerial contribution is to explain how solar radiation, risk aversion, and energy storage interact in the management of solar plants. First, a) plants sell in the spot market at night and store energy in the morning at the same time as electricity is purchased in the spot market; b) storage increases trading in futures and spot markets and creates value for generators. Second, regarding the use of options on solar radiation, we have shown that: a) the higher the total expected radiation, the higher (lower) the value of the call (put) option on radiation; b) the higher the call (put) price, the higher (lower) the generation and storage; c) the higher the expected

trading in the futures and spot markets, the higher the call, and the lower the put prices; d) the optimal strategy is to sell calls and buy put options; e) storage allows generators to sell more call options. Third, concerning risk aversion, we have shown that: a) a risk-averse generator expects to buy electricity in the spot market if and only if the expected production is less than the sales in the futures market; b) the higher the degree of risk aversion, the more a generator sells in the futures market and the higher the number of purchased put contracts. Finally, the comparison of the CSP and PV generation shows that the main qualitative insights are similar in both types of technology. Still, the PV is more profitable, has a lower risk of a significant loss, and the batteries create more value.

As future work, our model can be extended to better account for medium- and long-term trends that can potentially impact the market prices and the trading of forward contracts and financial options, conditioning the plant's profitability. These include political factors, new technological paradigms, and market regulations. This work can also be extended to analyze other generation technologies that combine a renewable input and the possibility of storage (e.g., wind, tides, and hydrogen).

Data Availability Statement

Data available on request from the authors.

References

Bhattacharya, S., Gupta, A., Kar, K., Owusu, A., 2020. Risk management of renewable power producers from co-dependencies in cash flows. European Journal of operational research 283, 1081–1093.

Bodie, Z., Kane, A., Marcus, A.J., 2014. Investments. volume 1. Tenth ed., McGraw-Hill.

Broadie, M., Detemple, J.B., 2004. Anniversary article: Option pricing: Valuation models and applications. Management science 50, 1145–1177.

Chen, Y., Billings, B.W., Powell, K.M., 2024. Industrial processes and the smart grid: Overcoming the variability of renewables by using built-in process storage and intelligent control strategies. International Journal of Production Research 62, 1686–1698.

Conejo, A.J., Carrión, M., Morales, J.M., et al., 2010. Decision making under uncertainty in electricity markets. volume 1. Springer.

DiOrio, N., Denholm, P., Hobbs, W.B., 2020. A model for evaluating the configuration and dispatch of pv plus battery power plants. Applied Energy 262, 114465.

Domínguez, R., Baringo, L., Conejo, A., 2012. Optimal offering strategy for a concentrating solar power plant. Applied Energy 98, 316 – 325.

Dowling, A.W., Zheng, T., Zavala, V.M., 2017. Economic assessment of concentrated solar power technologies: A review. Renewable and Sustainable Energy Reviews 72, 1019–1032.

EC Climate Action, 2022. European Commission, Directorate-General for Climate Action, 2050 long-term strategy. URL: https://ec.europa.eu/clima/eu-action/climate-strategies-targets/2050-long-term-strategy_en.

ECMWF Copernicus project, 2022. Climate Data Store. URL: https://cds.climate.copernicus.eu/cdsapp#!/home.

Elias, R., Wahab, M., Fang, L., 2014. A comparison of regime-switching temperature modeling approaches for applications in weather derivatives. European Journal of Operational Research 232, 549–560.

ESIOS, 2022. Red Eléctrica España. URL: https://www.esios.ree.es/es.

Fan, B., Liao, F., Yang, C., Qin, Q., 2023. Two-stage electricity production scheduling with energy storage and dynamic emission modelling. International Journal of Production Research , 1–20.

Feng, Y., Menezes, M.B., 2022. Integrated production and renewable energy generation in the presence of hydrogen energy storage. Production and Operations Management 31, 2222–2236.

Guajardo, J.A., 2018. Third-party ownership business models and the operational performance of solar energy systems. Manufacturing & Service Operations Management 20, 788–800.

Gutjahr, W.J., Kovacevic, R.M., Wozabal, D., 2022. Risk-averse bargaining in a stochastic optimization context. Manufacturing & Service Operations Management , Online.

Hannan, M., Wali, S., Ker, P., Abd Rahman, M., Mansor, M., Ramachandaramurthy, V., Muttaqi, K., Mahlia, T., Dong, Z., 2021. Battery energy-storage system: A review of technologies, optimization objectives, constraints, approaches, and outstanding issues. Journal of Energy Storage 42, 103023.

Hernández-Callejo, L., Gallardo-Saavedra, S., Alonso-Gómez, V., 2019. A review of photovoltaic systems: Design, operation and maintenance. Solar Energy 188, 426–440.

Hull, J.C., 1993. Options, Futures, and Other Derivative Securities. Prentice-Hall.

IRENA, 2022. Renewable power generation costs in 2022. International Renewable Energy Agency: Abu Dhabi .

IRENA, 2023. Renewable energy statistics 2023. International Renewable Energy Agency: Abu Dhabi .

Keles, D., Dehler-Holland, J., 2022. Evaluation of photovoltaic storage systems on energy markets under uncertainty using stochastic dynamic programming. Energy Economics 106, 105800.

Kök, A.G., Shang, K., Yücel, Ş., 2020. Investments in renewable and conventional energy: The role of operational flexibility. Manufacturing & Service Operations Management 22, 925–941.

Lai, C.S., Jia, Y., Lai, L.L., Xu, Z., McCulloch, M.D., Wong, K.P., 2017. A comprehensive review on large-scale photovoltaic system with applications of electrical energy storage. Renewable and Sustainable Energy Reviews 78, 439–451.

Leggio, K.B., 2007. Using weather derivatives to hedge precipitation exposure. Managerial Finance 33 (4), 246–252.

Li, L., Liu, J., Zhu, L., Zhang, X.B., 2020. How to design a dynamic feed-in tariffs mechanism for renewables–a real options approach. International Journal of Production Research 58, 4352–4366.

Luenberger, D., Ye, Y., 2008. Linear and Nonlinear Programming. volume 1. Springer Science.

Merzifonluoglu, Y., Uzgoren, E., 2018. Photovoltaic power plant design considering multiple uncertainties and risk. Annals of Operations Research 262, 153–184.

Oliveira, F.S., 2023. Procurement risk management in a petroleum refinery. Decision Sciences 54 (3), 277–296.

Oliveira, F.S., Ruiz, C., 2021. Analysis of futures and spot electricity markets under risk aversion. European Journal of Operational Research 291 (3), 1132–1148.

Peura, H., Bunn, D.W., 2021. Renewable power and electricity prices: the impact of forward markets. Management Science 67, 4772–4788.

REPowerEU, 2022. Communication from the commission to the european parliament, the european council, the council, the european economic and social committee and the committee of the regions. European Commission: Brussels, Belgium .

Rockafellar, R.T., Uryasev, S., 2002. Conditional value-at-risk for general loss distributions. Journal of Banking & Finance 26, 1443–1471.

Rockafellar, R.T., Uryasev, S., et al., 2000. Optimization of conditional value-at-risk. Journal of Risk 2, 21–42.

World Bank, 2021. Concentrating Solar Power: Clean Power on Demand 24/7. Washington, DC: World Bank.

APPENDIX

Appendix A. Notation

Indexes and Sets

a: Power flow from SF to ES ("$a = +$") or from ES to generate electricity ("$a = -$").
t: Hours of the day within the delivery day running from 1 to T.
ω: Scenarios running from 1 to Ω.
o: Identity of the option contract and its quantile.
$\mathbb{O}$: Set of the different types of options contracts available.
$\mathbb{D}$: Set of daylight hours within a day where $|\mathbb{D}| = D$.

Parameters

α: Proportion of observations on the left tail of the profit distribution.
$k_{t\omega}$: Generation cost at time t and scenario ω.
σ_o: Tick size, i.e., monetary unities per radiation unit.
η: Plant conversion efficiency from thermal power to electricity (p.u.).
β: Efficiency loss of storage (p.u.).
ρ^d: Total discount factor where d is the number of days from the present to the date of delivery of the contract, measured in fractions of the year.
$\widetilde{E}_{t\omega}$: Power generated by SF at time t and scenario ω.
h: Heliostat reflective area.
$\underline{b}$: Minimum energy content of ES.
$\bar{\bar{b}}$: Maximum energy content of ES.
$\bar{q}$: Maximum electric power output.
Δ: Maximum hourly power that can be transferred to/taken from ES.
$S_{t\omega}$: Spot price at time t and scenario ω.
F: Futures price.
c_o: Call option premium.
p_o: Put option premium.
R_ω: Average radiation in ω, computed over the corresponding times t where $o \in \mathbb{O}_t$.
R_o: Exercise radiation for option o.
$\breve{R}_{t\omega}$: observed solar radiation at hour t and scenario ω.

Variables

$\Pi^S_{t\omega}$: Spot market profit at time t, scenario ω.
Π_ω: Total profit at scenario ω.
q^F: Quantity traded in the futures market.
$q^S_{t\omega}$: Quantity traded by the generator in the spot market at time t in scenario ω.
q^c_o: Quantity purchased of call options.
q^p_o: Quantity purchase of put options.
$g_{t\omega}$: Power from SF to produce electricity, time t and scenario ω.
$\Delta_{at\omega}$: Power from SF to ES ($a = +$) or power from the ES to produce electricity ($a = -$), at time t and scenario ω.
$b_{t\omega}$: Energy available in ES, time t and scenario ω.
$E^C_{t\omega}$: Power curtailed from SF, time t and scenario ω.
ξ: Auxiliary variable equivalent to the Value-at-Risk (VaR) at optimality.
z_ω: Auxiliary variable required for CVaR formulation.

Appendix B. Lagrangian and KKT Conditions

Equation (B1) stands for the Lagrangian, $\mathcal{L}(.)$ of problem (1), in which the profit functions are
$\Pi_\omega = FDq^F - D\sum_{o\in\mathbb{O}}\left(q_o^c c_o + q_o^p p_o\right) + \rho^d D\sum_{o\in\mathbb{O}}\left(q_o^c\sigma_o\left(R_\omega - R_o\right)^+ + q_o^p\sigma_o\left(R_o - R_\omega\right)^+\right) + \rho^d\sum_t \Pi_{t\omega}^S$
and $\Pi_{t\omega}^S = S_{t\omega}q_{t\omega}^S - k_{t\omega}g_{t\omega}$.

$$
\begin{aligned}
\mathcal{L}(.) = {} & -\xi + \frac{1}{\alpha\Omega}\sum_\omega z_\omega + \\
& \sum_\omega \lambda_\omega\left(-z_\omega + \xi - \Pi_\omega\right) + \sum_\omega \Phi_\omega^z(-z_\omega) + \sum_{t\in\mathbb{D},\omega}\Phi_{t\omega}^S\left(q_{t\omega}^S - \eta\left(g_{t\omega} + \beta\Delta_{-t\omega}\right) + q^F\right) + \\
& \sum_{t\notin\mathbb{D},\omega}\Phi_{t\omega}^S\left(q_{t\omega}^S - \eta\left(g_{t\omega} + \beta\Delta_{-t\omega}\right)\right) + \sum_{t\in\mathbb{D},\omega}\Phi_{t\omega}^F\left(-q^F - q_{t\omega}^S\right) + \sum_{t\omega}\Gamma_{t\omega}^E\left(\widetilde{E}_{t\omega} - g_{t\omega} - \Delta_{+t\omega} - E_{t\omega}^C\right) + \\
& \sum_{(t>1)\omega}\Gamma_{t\omega}^B\left(b_{t\omega} - b_{t-1\omega} - \beta\Delta_{+t\omega} + \Delta_{-t\omega}\right) + \sum_\omega \Gamma_{1\omega}^B\left(b_{1\omega} - b_{T\omega} - \beta\Delta_{+1\omega} + \Delta_{-1\omega}\right) + \\
& \sum_{t\omega}\underline{\nu}_{t\omega}\left(\underline{b} - b_{t\omega}\right) + \sum_{t\omega}\overline{\nu}_{t\omega}\left(-\overline{b} + b_{t\omega}\right) + \sum_{at\omega}\delta_{at\omega}\left(\Delta_{at\omega} - \Delta\right) + \\
& \sum_{t\omega}\Phi_{t\omega}^q\left(\eta\left(g_{t\omega} + \beta\Delta_{-t\omega}\right) - \bar{q}\right) + \sum_{at\omega}\Phi_{at\omega}^\Delta\left(-\Delta_{at\omega}\right) + \sum_{t\omega}\Phi_{t\omega}^g\left(-g_{t\omega}\right) + \sum_{t\omega}\Phi_{t\omega}^E\left(-E_{t\omega}^C\right)
\end{aligned}
\tag{B1}
$$

The Karush-Kuhn-Tucker stationarity conditions (e.g., Luenberger and Ye 2008) are represented by the system of equations (B2):

$$\frac{\partial \mathcal{L}(.)}{\partial q^F} = 0 \iff -FD\sum_{\omega}\lambda_\omega + \sum_{t\in\mathbb{D},\omega}\Phi^S_{t\omega} - \sum_{t\in\mathbb{D},\omega}\Phi^F_{t\omega} = 0 \tag{B2a}$$

$$\frac{\partial \mathcal{L}(.)}{\partial q^S_{t\omega}} = 0 \iff -\rho^d\lambda_\omega S_{t\omega} + \Phi^S_{t\omega} - \Phi^F_{t\omega} = 0 \quad \forall t \in \mathbb{D}, \omega \tag{B2b}$$

$$\frac{\partial \mathcal{L}(.)}{\partial q^S_{t\omega}} = 0 \iff -\rho^d\lambda_\omega S_{t\omega} + \Phi^S_{t\omega} = 0 \quad \forall t \notin \mathbb{D}, \omega \tag{B2c}$$

$$\frac{\partial \mathcal{L}(.)}{\partial g_{t\omega}} = 0 \iff \rho^d\lambda_\omega k_{t\omega} - \Phi^S_{t\omega}\eta - \Gamma^E_{t\omega} + \Phi^q_{t\omega}\eta - \Phi^g_{t\omega} = 0 \qquad \forall t, \omega \tag{B2d}$$

$$\frac{\partial \mathcal{L}(.)}{\partial \Delta_{+t\omega}} = 0 \iff -\Gamma^E_{t\omega} - \beta\Gamma^B_{t\omega} + \delta_{+t\omega} - \Phi^\Delta_{+t\omega} = 0 \quad \forall t, \omega \tag{B2e}$$

$$\frac{\partial \mathcal{L}(.)}{\partial \Delta_{-t\omega}} = 0 \iff -\Phi^S_{t\omega}\eta\beta + \Gamma^B_{t\omega} + \delta_{-t\omega} + \Phi^q_{t\omega}\eta\beta - \Phi^\Delta_{-t\omega} = 0 \quad \forall t, \omega \tag{B2f}$$

$$\frac{\partial \mathcal{L}(.)}{\partial b_{t\omega}} = 0 \iff \Gamma^B_{t\omega} - \Gamma^B_{t+1\omega} - \underline{\nu}_{t\omega} + \overline{\nu}_{t\omega} = 0 \quad \forall t < T, \omega \tag{B2g}$$

$$\frac{\partial \mathcal{L}(.)}{\partial b_{T\omega}} = 0 \iff \Gamma^B_{T\omega} - \Gamma^B_{1\omega} - \underline{\nu}_{T\omega} + \overline{\nu}_{T\omega} = 0 \quad \forall \omega \tag{B2h}$$

$$\frac{\partial \mathcal{L}(.)}{\partial E^C_{t\omega}} = 0 \iff -\Gamma^E_{t\omega} - \Phi^E_{t\omega} = 0 \quad \forall t, \omega \tag{B2i}$$

$$\frac{\partial \mathcal{L}(.)}{\partial z_\omega} = 0 \iff \frac{1}{\alpha\Omega} - \lambda_\omega - \Phi^Z_\omega = 0 \quad \forall \omega \tag{B2j}$$

$$\frac{\partial \mathcal{L}(.)}{\partial \xi} = 0 \iff -1 + \sum_{\omega}\lambda_\omega = 0 \tag{B2k}$$

$$\frac{\partial \mathcal{L}(.)}{\partial q^c_o} = 0 \iff D\sum_{\omega}\lambda_\omega c_o - D\sum_{\omega}\rho^d\lambda_\omega\sigma_o\left(R_\omega - R_o\right)^+ = 0 \quad \forall o \tag{B2l}$$

$$\frac{\partial \mathcal{L}(.)}{\partial q^p_o} = 0 \iff D\sum_{\omega}\lambda_\omega p_o - D\sum_{\omega}\rho^d\lambda_\omega\sigma_o\left(R_o - R_\omega\right)^+ = 0 \quad \forall o \tag{B2m}$$

Appendix C. Proof of Analytical Results

Proof. Proof of Lemma 4.1: From the KKT condition (B2k) we know that $\sum_\omega \lambda_\omega = 1$. Moreover, from the KKT condition (B2j), it is known that $\lambda_\omega + \Phi^Z_\omega = \frac{1}{\alpha\Omega}$. a) Therefore, when $z_\omega > 0$ the tail constraint is binding and $\lambda_\omega = \frac{1}{\alpha\Omega}$ and $\Phi^Z_\omega = 0$. b) As when both (1d) and (1e) are binding $z_\omega = 0$ and $\xi = \Pi_\omega$ then $\lambda_\omega \leq \frac{1}{\alpha\Omega}$ and $\Phi^Z_\omega \leq \frac{1}{\alpha\Omega}$. □

Proof. Proof of Lemma 4.2: From the KKT condition (B2l) it is known that for all hour t in which a call contract is available (daylight time), $t \in \mathbb{D}$, $\sum_{t\in\mathbb{D}}\sum_\omega \lambda_\omega c_o - \sum_{t\in\mathbb{D}}\sum_\omega \rho^d\lambda_\omega\sigma_o\left(R_\omega - R_o\right)^+ = 0$. Furthermore, by the KKT condition (B2m), it is known that for all hours o in which a put contract is available $\sum_{t\in\mathbb{D}}\sum_\omega \lambda_\omega p_o - \sum_{t\in\mathbb{D}}\sum_\omega \rho^d\lambda_\omega\sigma_o\left(R_o - R_\omega\right)^+ = 0$. Then, by letting D be the number of hours in which the option contract is traded, and as $\sum_\omega \lambda_\omega = 1$, these two conditions simplify to $c_o - \rho^d\sum_\omega \lambda_\omega\sigma_o\left(R_\omega - R_o\right)^+ = 0$ and $p_o - \rho^d\sum_\omega \lambda_\omega\sigma_o\left(R_o - R_\omega\right)^+ = 0$. Moreover, it follows from equations (5) that the risk premiums are such that $c_o -$

$\frac{\rho^d}{\Omega}\sum_\omega \sigma_o (R_\omega - R_o)^+ = 0$ and $p_o - \frac{\rho^d}{\Omega}\sum_\omega \sigma_o (R_o - R_\omega)^+ = 0$. Hence, in the optimum, for the call contract, $\frac{\rho^d}{\Omega}\sum_\omega \sigma_o (R_\omega - R_o)^+ = \rho^d \sum_\omega \lambda_\omega \sigma_o (R_\omega - R_o)^+$ which is equivalent to $\sum_\omega \lambda_\omega (R_\omega - R_o)^+ = \frac{1}{\Omega}\sum_\omega (R_\omega - R_o)^+$. Moreover, as for the scenarios where ω is in the tail, ω^z, $\lambda_\omega = \frac{1}{\alpha\Omega}$ then $\frac{1}{\alpha\Omega}\sum_{\omega^z} (R_{\omega^z} - R_o)^+ = \frac{1}{\Omega}\sum_\omega (R_\omega - R_o)^+$ from which we get $\sum_{\omega^z} (R_{\omega^z} - R_o)^+ = \alpha \sum_\omega (R_\omega - R_o)^+$. Similarly, for the put option, it follows that $\rho^d \sum_\omega \lambda_\omega \sigma_o (R_o - R_\omega)^+ = \frac{\rho^d}{\Omega}\sum_\omega \sigma_o (R_o - R_\omega)^+$, which is equivalent to $\sum_\omega \lambda_\omega (R_o - R_\omega)^+ = \frac{1}{\Omega}\sum_\omega (R_o - R_\omega)^+$, from which it follows $\sum_{\omega^z} (R_o - R_{\omega^z})^+ = \alpha \sum_\omega (R_o - R_\omega)^+$. □

Proof. Proof of Proposition 4.3: It follows from equations (5) that from the non-arbitrage condition, the risk premiums are such that $c_o = \frac{\rho^d}{\Omega}\sum_\omega \sigma_o (R_{o\omega} - R_o)^+$ and $p_o = \frac{\rho^d}{\Omega}\sum_\omega \sigma_o (R_o - R_{o\omega})^+$. Then, the call price is equal to or greater than the put price if and only if $\frac{\rho^d}{\Omega}\sum_\omega \sigma_o (R_{o\omega} - R_o)^+ \geq \frac{\rho^d}{\Omega}\sum_\omega \sigma_o (R_o - R_{o\omega})^+$ and hence $\sum_\omega (R_{o\omega} - R_o)^+ \geq \sum_\omega (R_o - R_{o\omega})^+$, which is equivalent to $\sum_{\omega^+} R_{o\omega^+} \geq \sum_{\omega^-} R_{o\omega^-}$. □

Proof. Proof of Proposition 4.4: At hour $t \in \mathbb{D}$, the quantities traded in the spot and forward market are determined by equation (1f), $q^F + q^S_{t\omega} \leq \eta (g_{t\omega} + \beta\Delta_{-t\omega})$, with the respective dual variable $(\Phi^S_{t\omega})$, and equation (1h), $-q^F \leq q^S_{t\omega}$, with a dual variable $(\Phi^F_{t\omega})$. Additionally, from equation (B2b), it is known that $-\rho^d\lambda_\omega S_{t\omega} + \Phi^S_{t\omega} - \Phi^F_{t\omega} = 0$, which is equivalent to $\rho^d\lambda_\omega S_{t\omega} = \Phi^S_{t\omega} - \Phi^F_{t\omega}$. For any scenario ω in the tail of the profit function $\lambda_\omega > 0$ and consequently $\rho^d\lambda_\omega S_{t\omega} > 0$, and $\Phi^S_{t\omega} - \Phi^F_{t\omega} > 0$. This means that, when equation (1h) is binding so is (1f); but (1f) can be binding when equation (1h) is not. Therefore, it follows that for any scenario considered for the calculation of the expected value $q^F + q^S_{t\omega} = \eta (g_{t\omega} + \beta\Delta_{-t\omega})$. Then $q^S_{t\omega} < 0$ if and only if $\eta (g_{t\omega} + \beta\Delta_{-t\omega}) < q^F$. By taking the expectation over these scenarios it follows that $\frac{1}{\Omega}\sum_\omega q^S_{t\omega} < 0$ if and only if $\frac{\eta}{\Omega}\sum_\omega (g_{t\omega} + \beta\Delta_{-t\omega}) < \frac{1}{\Omega}\sum_\omega q^F$. This is equivalent to $q^F > \frac{\eta}{\Omega}\sum_\omega (g_{t\omega} + \beta\Delta_{-t\omega})$. □

Proof. Proof of Proposition 4.5: From the same arguments used in Proposition 4.4, for an hour $t \in \mathbb{D}$, let constraint (1f) be binding, i.e., $q^F + q^S_{t\omega} = \eta (g_{t\omega} + \beta\Delta_{-t\omega})$. This is equivalent to $\lambda_\omega \left(q^F + q^S_{t\omega}\right) = \lambda_\omega \eta (g_{t\omega} + \beta\Delta_{-t\omega})$. It then follows that $\sum_\omega \lambda_\omega \left(q^F + q^S_{t\omega}\right) = \sum_\omega \lambda_\omega \eta (g_{t\omega} + \beta\Delta_{-t\omega})$, and as $\sum_\omega \lambda_\omega = 1$, then $q^F + \sum_\omega \lambda_\omega q^S_{t\omega} = \sum_\omega \lambda_\omega \eta (g_{t\omega} + \beta\Delta_{-t\omega})$. Then, by summing over all the daylight hours ($t \in \mathbb{D}$), and all the ω scenarios, we get $Dq^F + \sum_{t\in\mathbb{D},\omega} \lambda_\omega q^S_{t\omega} = \sum_{t\in\mathbb{D},\omega} \lambda_\omega \eta (g_{t\omega} + \beta\Delta_{-t\omega})$, and consequently $q^F = \frac{\eta}{D}\sum_{t\in\mathbb{D},\omega} \lambda_\omega (g_{t\omega} + \beta\Delta_{-t\omega}) - \frac{1}{D}\sum_{t\in\mathbb{D},\omega} \lambda_\omega q^S_{t\omega}$. Moreover, as from Proposition 4.1, if $z_\omega > 0$ then $\lambda_\omega = \frac{1}{\alpha\Omega}$, it follows that $q^F = \frac{\eta}{D\alpha\Omega}\sum_{t\in\mathbb{D},\omega^z} (g_{t\omega^z} + \beta\Delta_{-t\omega^z}) - \frac{1}{D\alpha\Omega}\sum_{t\in\mathbb{D},\omega^z} q^S_{t\omega^z}$. □

Proof. Proof of Proposition 4.6: From Proposition 4.5, $q^F = \frac{\eta}{D\alpha\Omega}\sum_{t\in\mathbb{D},\omega^z} (g_{t\omega^z} + \beta\Delta_{-t\omega^z}) - \frac{1}{D\alpha\Omega}\sum_{t\in\mathbb{D},\omega^z} q^S_{t\omega^z}$. Then $q^F_1 = \frac{\eta}{D\alpha\Omega}\sum_{t\in\mathbb{D},\omega^z} (g_{t\omega^z} + \beta\Delta_{-t\omega^z}) - \frac{1}{D\alpha\Omega}\sum_{t\in\mathbb{D},\omega^z} q^S_{t\omega^z}$ and $q^F_0 = \frac{\eta}{D\alpha\Omega}\sum_{t\in\mathbb{D},\omega^z} g_{t\omega^z} - \frac{1}{D\alpha\Omega}\sum_{t\in\mathbb{D},\omega^z} q^S_{t\omega^z}$. Let the solar field's production level and the expected spot trading be independent of storage ownership. Then, as from the KKT (B2j), we know that $\lambda_\omega = \frac{1}{\alpha\Omega}$, it follows that $q^F_1 - q^F_0 = \frac{\eta}{D\alpha\Omega}\sum_{t\in\mathbb{D},\omega^z} \beta\Delta_{-t\omega^z}$. Hence, $q^F_1 - q^F_0$ increases as α converges to 0, i.e., the generator degree of risk aversion increases. □

Proof. Proof of Proposition 4.7: At daylight hour $t \in \mathbb{D}$, from the same arguments used in Proposition 4.4, let constraint (1f) be binding, i.e., $q^F + q^S_{t\omega} = \eta\,(g_{t\omega} + \beta\Delta_{-t\omega})$. This is equivalent to $q^S_{t\omega} = \eta\,(g_{t\omega} + \beta\Delta_{-t\omega}) - q^F$. Hence, for a given q^F, the higher $\Delta_{-t\omega}$ the higher $q^S_{t\omega}$. □

Proof. Proof of Proposition 4.8: From identities (2) and (3), $R_\omega = \frac{1}{D}\sum_{t\in\mathbb{D}} \breve{R}_{t\omega}$ and $\widetilde{E}_{t\omega} = h\breve{R}_{t\omega}$. Consequently, as $\breve{R}_{t\omega} = \frac{\widetilde{E}_{t\omega}}{h}$, it then follows that $R_\omega = \frac{1}{hD}\sum_{t\in\mathbb{D}} \widetilde{E}_{t\omega}$. From equations (5a) and (5b) it follows $c_o = \frac{\rho^d}{\Omega}\sum_\omega \sigma_o\,(R_\omega - R_o)^+$ and $p_o = \frac{\rho^d}{\Omega}\sum_\omega \sigma_o\,(R_o - R_\omega)^+$, and equivalently $c_o = \frac{\rho^d}{\Omega}\sigma_o \sum_\omega \left(\frac{1}{hD}\sum_{t\in\mathbb{D}} \widetilde{E}_{t\omega} - R_o\right)^+$ and $p_o = \frac{\rho^d}{\Omega}\sigma_o \sum_\omega \left(R_o - \frac{1}{hD}\sum_{t\in\mathbb{D}} \widetilde{E}_{t\omega}\right)^+$. □

Proof. Proof of Proposition 4.9: From Proposition 4.8 we know that $c_o = \frac{\rho^d}{\Omega}\sigma_o \sum_\omega \left(\frac{1}{hD}\sum_{t\in\mathbb{D}} \widetilde{E}_{t\omega} - R_o\right)^+$ and $p_o = \frac{\rho^d}{\Omega}\sigma_o \sum_\omega \left(R_o - \frac{1}{hD}\sum_{t\in\mathbb{D}} \widetilde{E}_{t\omega}\right)^+$. Next, assuming that the spillage is zero, i.e., as it is the case when the system is optimally used, then $E^C_{t\omega} = 0$ and from equation (1i) it is known that $\widetilde{E}_{t\omega} = g_{t\omega} + \Delta_{+t\omega}$. Consequently, it follows that $c_o = \frac{\rho^d}{\Omega}\sigma_o \sum_\omega \left(\frac{1}{hD}\sum_{t\in\mathbb{D}} (g_{t\omega} + \Delta_{+t\omega}) - R_o\right)^+$ and $p_o = \frac{\rho^d}{\Omega}\sigma_o \sum_\omega \left(R_o - \frac{1}{hD}\sum_{t\in\mathbb{D}} (g_{t\omega} + \Delta_{+t\omega})\right)^+$. Let ω^+ (ω^-) stand for the subset of scenarios in which the call (put) is valuable. Then we can equivalently calculate these prices as $c_o = \frac{\rho^d\sigma_o}{\Omega}\sum_{\omega^+}\left(\frac{1}{hD}\sum_{t\in\mathbb{D}} (g_{t\omega} + \Delta_{+t\omega}) - R_o\right)$ and $p_o = \frac{\rho^d\sigma_o}{\Omega}\sum_{\omega^-}\left(R_o - \frac{1}{hD}\sum_{t\in\mathbb{D}} (g_{t\omega} + \Delta_{+t\omega})\right)$. These equations simplify to
$c_o = \frac{\rho^d\sigma_o}{\Omega}\sum_{\omega^+}\frac{1}{hD}\sum_{t\in\mathbb{D}} (g_{t\omega} + \Delta_{+t\omega}) - \frac{\rho^d\sigma_o}{\Omega}\sum_{\omega^+} R_o$ and
$p_o = \frac{\rho^d\sigma_o}{\Omega}\sum_{\omega^-} R_o - \frac{\rho^d\sigma_o}{\Omega}\frac{1}{hD}\sum_{\omega^-}\sum_{t\in\mathbb{D}} (g_{t\omega} + \Delta_{+t\omega})$. Then, as the number of scenarios in the tail is $\alpha\Omega$, these equations are equivalent to: $c_o = \frac{\rho^d\sigma_o}{hD\Omega}\sum_{\omega^+}\sum_{t\in\mathbb{D}} (g_{t\omega} + \Delta_{+t\omega}) - \alpha\rho^d\sigma_o R_o$ and $p_o = \alpha\rho^d\sigma_o R_o - \frac{\rho^d\sigma_o}{hD\Omega}\sum_{\omega^-}\sum_{t\in\mathbb{D}} (g_{t\omega} + \Delta_{+t\omega})$. For this reason, we can obtain the relationship between electricity generated and stored and the option prices in a day as: $\frac{\rho^d\sigma_o}{hD\Omega}\sum_{\omega^+}\sum_{t\in\mathbb{D}} (g_{t\omega} + \Delta_{+t\omega}) = c_o + \alpha\rho^d\sigma_o R_o$ and $\frac{\rho^d\sigma_o}{hD\Omega}\sum_{\omega^-}\sum_{t\in\mathbb{D}} (g_{t\omega} + \Delta_{+t\omega}) = \alpha\rho^d\sigma_o R_o - p_o$. □

Proof. Proof of Proposition 4.10: From Proposition 4.1, if $z_\omega > 0$ then $\lambda_\omega = \frac{1}{\alpha\Omega}$. Moreover, from the objective function (1b) and (1c), $\Pi_\omega = FDq^F - D\sum_{o\in\mathbb{O}} (q^c_o c_o + q^p_o p_o) + \rho^d D\sum_{o\in\mathbb{O}} \left(q^c_o\sigma_o\,(R_\omega - R_o)^+ + q^p_o\sigma_o\,(R_o - R_\omega)^+\right) + \rho^d\sum_t \left(S_{t\omega}q^S_{t\omega} - k_{t\omega}g_{t\omega}\right)$. Then the risk-averse expected profit is obtained by multiplying (1b) by λ_ω and summing over the scenarios: $\mathbb{E}(\Pi) = FDq^F - D\sum_{o\in\mathbb{O}} (q^c_o c_o + q^p_o p_o) + \frac{\rho^d D}{\alpha\Omega}\sigma_o\sum_\omega\sum_{o\in\mathbb{O}} \left(q^c_o\,(R_\omega - R_o)^+ + q^p_o\,(R_o - R_\omega)^+\right) + \frac{\rho^d}{\alpha\Omega}\sum_{t\omega}\left(S_{t\omega}q^S_{t\omega} - k_{t\omega}g_{t\omega}\right)$. As q^F, q^c_o, q^p_o, are all decided at time zero, based on the risk-averse expected radiation, spot prices, generation from the solar field, TES discharge, and production costs, then only the options trading needs to be determined to maximize the expected trading profit, which from the expected total profit, for option o, and given that the tail profits are in scenarios, ω^z, is equal to $\mathbb{E}(\Pi_o) = -D\,(q^c_o c_o + q^p_o p_o) + \frac{\rho^d D}{\alpha\Omega}\sigma_o\sum_{\omega^z}\left(q^c_o\,(R_{\omega^z} - R_o)^+ + q^p_o\,(R_o - R_{\omega^z})^+\right)$. The optimal $\mathbb{E}(\Pi_o)$ is also obtained by maximizing the average option profit per hour $\mathbb{E}(\Pi^{t\in\mathbb{D}}_o) = -q^c_o c_o - q^p_o p_o + \frac{\rho^d}{\alpha\Omega}\sigma_o\sum_{\omega^z} q^c_o\,(R_{\omega^z} - R_o)^+ + \frac{\rho^d}{\alpha\Omega}\sigma_o\sum_{\omega^z} q^p_o\,(R_o - R_{\omega^z})^+$, which is equivalent to: $\mathbb{E}(\Pi^{t\in\mathbb{D}}_o) = q^c_o\left(\frac{\rho^d\sigma_o}{\alpha\Omega}\sum_{\omega^z}(R_{\omega^z} - R_o)^+ - c_o\right) + q^p_o\left(\frac{\rho^d\sigma_o}{\alpha\Omega}\sum_{\omega^z}(R_o - R_{\omega^z})^+ - p_o\right)$. As from Proposition 4.2, for the scenarios ω^z in the tail of the distribution, for

the call option $\sum_{\omega^z}(R_{\omega^z}-R_o)^+ = \alpha\sum_{\omega}(R_\omega-R_o)^+$, and for the put option, $\sum_{\omega^z}(R_o-R_{\omega^z})^+ = \alpha\sum_{\omega}(R_o-R_\omega)^+$, it then follows that, equivalent we get: $\mathbb{E}(\Pi_o^{t\in\mathbb{D}}) = q_o^c\left(\frac{\rho^d\sigma_o}{\alpha\Omega}\alpha\sum_{\omega}(R_\omega-R_o)^+ - c_o\right) + q_o^p\left(\frac{\rho^d\sigma_o}{\alpha\Omega}\alpha\sum_{\omega}(R_o-R_\omega)^+ - p_o\right)$. As from identities (5a) and (5b), $c_o = \frac{\rho^d}{\Omega}\sum_{\omega}\sigma_o(R_\omega-R_o)^+$ and $p_o = \frac{\rho^d}{\Omega}\sum_{\omega}\sigma_o(R_o-R_\omega)^+$, it follows that: $\mathbb{E}(\Pi_o^{t\in\mathbb{D}})=0$. □